Differentiating Human iPSCs into Dopaminergic Neurons that Express Classical Biochemical Traits and Show Neuronal Transmission and Excitability

Differentiating Human iPSCs into Dopaminergic Neurons that Express Classical Biochemical Traits and Show Neuronal Transmission and Excitability

Vinicius Sanz

A Thesis in the Field of Biology

for the Degree of Master of Liberal Arts in Extension Studies

Harvard University

May 2022

Abstract

Parkinson's disease (PD) is an incurable neurodegenerative disorder. Current therapeutic approaches are aimed to lessen the symptoms without slowing or halting the disease progression (Hammond, Constance et al., 2007).

Models that allow to study the cellular and molecular mechanisms behind the neurological dysfunction are critical in developing new therapies. In vitro neuronal models have been used to recapitulate patient pathophysiology. However, it is crucial to choose the correct cell population to study the disease of interest. iPSC cellular models have the advantage of recapitulating the patient's own cellular background and for this reason they are considered the best model for generating disease-relevant neurons.

Here we optimized a protocol to differentiate iPSC in mid-dopaminergic neurons (mDA, the cells affected by PD) and performed different assays to test the level of differentiation and neuronal phenotype.

We tested samples from the 5 differentiation stages in our protocol and observed expression of both early and late classical dopaminergic neuronal markers such as SHH, FGF8, FOXA2, LMX1A, NURR1, TUBB and TH.

To further characterize the maturation of our neuronal network upon differentiation of cells from neurospheres, we measured neuronal activity by using multi electrode array and calcium influx assay. Our data showed that the mean firing rate of iPSC-derived mDA increased from < 0.04 Hz at day 9, to 2.43 Hz by day 20. The number

of spikes also increased from < 38 on day 5, to 2196 spikes on day 20, demonstrating action potentials are spontaneously being fired by the plated neurons.

Finally we observed that dysregulation of calcium influx in mature mDA neurons upon treatment with receptor agonists leads to cell death, as seen by the decrease in TH levels.

Taken together the results we report here show we can efficiently differentiate human iPSCs in mature and active dopaminergic neurons and this model may be potentially used for further investigation of therapies against PD.

Acknowledgments

First, I would like to thank my thesis director, Dr. Mirko Messa. Dr. Messa provided an immeasurable amount of support and guidance during this master's program that has culminated in my thesis project. Secondly, I would like to thank Mary Dovlatyan, who assisted me greatly in my experiments and provided guidance in some of the assays performed in my thesis. Lastly, I would like to thank my research advisor at Harvard, Dr. James Morris. His feedback and insights were crucial for me to complete this project.

Table of Contents

List of Tables

List of Figures

Chapter I.

Introduction

PD is a neurodegenerative disorder, affecting over 10 million people around the globe according to The American Parkinson Disease Association (APDA). PD is the second most common neurodegenerative disorder after Alzheimer's disease, it is a debilitating and incurable disease, and currently 1-3% of individuals who are over the age of 60 are PD patients (Ball, Nicole et al., 2019). This disorder is characterized by the loss of dopaminergic neurons in the brain, specifically located in the substantia nigra of the midbrain region. Dopaminergic neurons are responsible for controlling voluntary motor movement, and their loss typically leads to well-known PD symptoms such as stiffness, trembling, rigidity of the muscles and the slowness of movement also known as bradykinesia, which is one of the early signs observed in PD (Berardelli, A et al., 2001). Motor symptoms are not the only symptoms affected by this disorder; non-motor effects such as depression, anxiety, cognitive decline, rapid eye movement, behavioral sleep disorder, constipation, and other behavioral disturbances also affect patients. Due to motor and non-motor symptoms, PD patients' quality of life is reduced greatly, making it very difficult to manage day-to-day demands. Current medications are centered on dopamine replacement since the hallmark of the disease is the loss of dopaminergic neuronal function in addition to electrode treatment for deep brain stimulation (Hammond, Constance et al., 2007). However, these therapeutic approaches can only lessen the symptoms without

slowing or halting the disease progression. Thus, the importance of finding a therapy that can stop the disease progression and improve patient life is crucial.

Dopaminergic Neurons

Dopaminergic neurons are found in the midbrain region of the basal ganglia circuitry. The basal ganglia are not a single structure but a collection of structures that are collectively called the basal ganglia. The three main nuclei regions of the basal ganglia are the globus pallidus, and the caudate and putamen that collectively are called the striatum. The striatum forms a loop with the substantia nigra, in the midbrain region, to link the cortex with the upper motor neurons. This collection of structures is responsible for motor control as well as other voluntary behaviors (Yin et al., 2006). The substantia nigra is one of the main regions that produces dopamine and plays an important role in modulating motor movement. The dopaminergic neurons of the substantia nigra projects and synapses in multiple regions of the basal ganglia, but it does more specifically to the putamen of the striatum, forming the nigrostriatal dopamine pathway. This pathway contains 80% of dopamine produced in the brain. The striatum contains two receptors in which the substantia nigra synapse, the D1 and D2 receptors. Clinical studies have shown that activating the D2 receptor is beneficial in the treatment of PD (Le et al., 2001). PD is characterized by the loss of dopaminergic neurons in the substantia nigra, given the importance of the nigrostriatal dopamine pathway in dopamine production, this pathway is critically involved in the motor deficit seen in PD.

The mechanism that is causing the loss of dopaminergic neurons is poorly understood; however, multiple lines of research suggest a combinatory role for both genetic and environmental factors. Current studies have been focusing on key components that are

thought to lead to PD, such as the aggregation of misfolded alpha-synuclein (α-syn), mitochondria dysfunction, and lysosome dysfunction (Ball, Nicole et al., 2019).

Alpha – synuclein

Alpha-synuclein is one of the key elements linked to the development of PD. It is an abundant protein located in the presynaptic axon terminal, which is a specialized area of the neuron that contains the neurotransmitters, the body's chemical messengers. The aggregation of misfolded α-syn leads to the formation of inclusions known as Lewy-bodies, which are known to develop inside dopaminergic neurons in PD (Mellier et al., 2020). Multiple studies have shown that α-syn is naturally found in the cytosol in an unfolded form that is not toxic (Burré et al., 2015). However, upon taking an oligomers and fibrils form, α-syn forms aggregates, Lewy-bodies are formed and induces cellular toxicity leading to the disruption of synaptic-vesicle motility and dopamine release (Outeiro et al., 2008). The formation of aggregates has also been linked to A53T point mutation and a mutation of the gene encoding for α-syn, SNCA. This suggests that both environmental and genetic factors play a role in the formation of α-syn aggregates linked to PD. Interestingly, α-syn has also been linked to mitochondrial dysfunction, another key important element connected to PD, where pathogenic α-syn induces mitochondrial fragmentation and reactive oxygen species (ROS) production *in vitro* and *in vivo* (Ryan, Brent J et al., 2015).

Mitochondria Dysfunction

Mitochondria dysfunction is associated with PD pathogenesis. One strong piece of evidence linked to mitochondria dysfunction is from a study where they observed in PD patients, a high level of mitochondria DNA deletion in the substantia nigra (Bender, Andreas et al, 2006). Mitochondrial autophagy, known as mitophagy, is the mitochondrial quality control mechanism that enables the degradation of defective mitochondria following damage or stress by autophagy. Mitophagy sustains mitochondrial network homeostasis. When there is dysfunction in the process of mitophagy, there is an accumulation of defective mitochondria in the brain over the being's lifetime, leading to the increased formation of oxidative stress, loss of ATP, and eventually cell death (Park, Jin-Sung et al., 2018).

Defective mitophagy is linked to two important familial PD genes: Parkin RBR E3 ubiquitin-protein ligase (PARKIN) and PTEN-induced kinase 1 (PINK1). These two genes are key components in the activation of mitophagy. Upon mitochondrial depolarization, protein kinase Pink1 (constitutively imported into the mitochondria) is recruited and accumulates on the outer mitochondrial membrane. In succession, Pink1 recruits the E3 ubiquitin ligase Parkin from the cytosol and phosphorylates it, activating Parkin. Once activated, Parkin translocate to the damaged outer mitochondrial membrane, which in turn ubiquitylate substrates on the outer mitochondrial membrane, such as Translocase of Outer Mitochondrial Membrane 20 (TOMM20) protein. Once TOMM20 is tagged with ubiquitin to be degraded, the damaged mitochondria are taken up by the lysosome and degraded. Given the importance of these two genes to mitochondrial homeostasis, a mutation in either

of the genes will lead to the impairment of mitophagy function (Narendra, Derek et al., 2009).

Unless the dysfunctional mitochondria are eliminated, PD will eventually arise. Drugs that can activate PARKIN or PINK1, for example, circumventing the mutation which isn't allowing mitophagy to take place to eliminate the dysfunctional mitochondria, would be one of the solutions to fight PD. Thus, the importance of having a great cellular model to study the effect of these types of drugs is imperative.

Lysosomal Dysfunction

Like α-syn and mitochondria, lysosomal dysfunction has also been linked to PD. The lysosome plays an important role in maintaining neuronal homeostasis (Navarro-Romero, Alba et al., 2020), their main function being the degradation of intracellular and extracellular macromolecules. Lysosome dysfunction can happen as the result of a mutation in the GBA gene that encodes for lysosomal enzyme β-glucocerebrosidase (GCase), and ATP13A2 which encodes for lysosomal ATPase (Ramirez, Alfredo et al., 2006). Upon mutation of such genes, the lysosome stops functioning properly and now the elimination of dysfunctional mitochondria may be impacted, and proteins such as α-syn that are maintained by the lysosome can reach high concentrations, resulting in the formation of aggregates and Lewy-bodies inclusions, consequently causing the degeneration of dopaminergic neurons (Behl, Tapan et al., 2021).

Finding a system that allows to better study the dysfunctions and aggregations mentioned previously is critical in developing new medications and therapies. While biochemical models are used to study the binding or activity of a biological molecule, cellular models are the representation of the actual cellular environment, acting as an

intermediate between biochemical screens and the capacity to predict *in vivo* effects. Thus, cellular models will give key information during the drug discovery process. Examples of such information are:

- Understand the mechanism of action (MOA), such as the drug activation of a particular pathway of interest
- Identify other targets in the pathway of interest
- Determine the pharmacodynamics of the drug such as selecting the ideal dose range to be used *in vivo* models
- Evaluate the potency and toxicity of the drug (Michelini, Elisa et al., 2010).

Cellular Models

Given the importance of cellular models for developing drugs and to understand the pathophysiological mechanisms causing the disease, the importance of choosing the right cellular model that will provide the information necessary to respond key questions while tackling a disease of interest is clear. When choosing the cellular model, it needs to be taken into consideration what is the best type of cells, species and cell availability for the disease of interest. When looking at cellular models, the most frequent used are primary cells, immortalized cells, and Induced Pluripotent Stem Cell (iPSC). Primary cellular models are taken directly from the tissue through enzymatic or mechanical measures and optimized under culture conditions. The main advantage of using primary cells is that they mirror the cellular environment found *in vivo*. However, it is often difficult to obtain the proper primary cultures, especially for diseases that uses brain as their focus of study since you require fresh samples. Primary cultures have a low *in vitro* proliferative capacity, and

the isolation protocol may be cumbersome (Kaur et al., 2012). Another option consists of utilizing immortalized cellular models, either tumorous cells that do not stop dividing or cells that have been manipulated to proliferate indefinitely *in vitro* (immortalized cell cultures). The advantages of using immortalized cells are their ability to grow indefinitely and that they are cost and time effective. However, their major disadvantage is the lack of characteristics and functions of the native cell (Maqsood, Muhammad Irfan et al., 2013). The iPSC cellular model is derived by reprogramming somatic cells to a pluripotent state, through the overexpression of a key set of transcription factors. The advantage of using iPSCs are their ability to be pluripotent, meaning they can become any differentiated cell in the human body, they do not require destruction of embryos, thus circumventing ethical considerations, and they can be patient-specific, which can be easily derived from a variety of genetic backgrounds (individual patients), preventing immune rejections, and allowing novel studies of heritable genetic disorders in their human cell types. Most importantly, iPSCs reflect *in vivo* physiological or pathological conditions. iPSC's can also be used for potential cell replacement therapies. The disadvantages of using iPSCs are the possibility of generating non-homogenous cell populations, long and complex differentiation protocols that can go from weeks to months, and there is a low efficacy yield in comparison with the other two models (Ebert, Antje D et al, 2012).

Due to the iPSC cellular model containing the patient's own cellular background, it is deemed the best model for generating dopaminergic neurons, since this model is able to emulate the correct cellular environment of dopaminergic neurons in PD. Primary cellular models also have the ability to reflect an *in vivo* environment like iPSCs; however due to the necessity of having to perform numerous experiments, it would require too many

invasive fresh harvests from either mice or humans, thus not an ideal model to be used in PD. As one might expect, immortalized cellular models would not be an ideal model to be used in this scenario, for the lack of ability to mimic the actual environment of dopaminergic neurons due to having a mutagenized genome with unlimited proliferative capabilities.

Can we optimize a protocol to differentiate iPSCs in dopaminergic neurons that express classical biochemical traits and show neuronal excitability and transmission? Can we optimize a protocol to differentiate iPSCs in dopaminergic neurons that express classical biochemical traits and show neuronal excitability and transmission? The importance of optimizing and characterizing an assay not only tells us the assay is good enough, but also reassures the assay was thoroughly studied, the data generated is reproducible and a conclusion can be drawn, avoiding bottlenecks to be reached. We will analyze the early stages of iPSC stem cell differentiation to identify early proliferating dopaminergic progenitor cells such as secreted signaling proteins, sonic hedgehog (Shh) and fibroblast growth factor 8 (Fgf8), and post-mitotic dopaminergic transcription factor Nurr1. However, even if we can detect early proliferating dopaminergic progenitor cells in initial experiments, as is common in iPSC stem cell differentiation, there will be a sub-population of cells that won't be neuronal and dopaminergic cells, and a possibility that the percentage of dopaminergic cells population will be low, which would render this cell model ineffective. To further characterize this cellular model, the next step is to identify the percentage of the dopaminergic neuron population that is formed, identified through determining expression of the neuronal marker tyrosine hydroxylase (TH) in TUBβIII neurons.

If results are positive, we will then characterize the functionality of the iPSC neurons through mass spectroscopy on culture media to detect release of dopamine. As a second functional indication, we will perform electrophysiological recording of signals from neuronal cultures plated on multi electrode array (MEA) plates.

There is a need for better models to be able to replicate the pathological process underlying the dopaminergic neuron degeneration observed in PD. By optimizing and characterizing a protocol to differentiate iPSCs into dopaminergic neurons that express classical biochemical traits and show neuronal excitability and transmission, we will help scientists take a step forward towards a treatment for one of the biggest unmet medical needs burdening our society.

Chapter II.

Materials and Methods

mDA Differentiation

To begin differentiation a 6-well dish was coated with VTN and incubated for 1 hour at 37ºC. Human stem cell 8402 was then plated at a density of 200,000 cells per well and incubated at 37ºC, 5% CO_2 (Day 0). Media was switched every other day. Once cells reached 70% confluence, media was change to Phase I media (Table 13), and hemi-fed every other day for a period of 7 days. On day 8 cells were suspended using Accutase, plated 400,000 cells/well in a 96-well ULA plate using Phase II media (Table 14). Cells were incubated 37ºC, 5% CO_2 for a period of 7 days. Neurospheres began forming during Phase II in each well, consequently, to avoid disturbing neurospheres, media was not changed during this period. On day 15 Phase III then took place. Neurospheres were pooled and placed in a Corning 125ml Spinner flask and waited until Neurospheres were settled to switch to Phase III media (Table 15), then placed on spinner incubator at 37ºC, 5% CO_2 at a speed of 60rpm for 7 days. No media change during Phase III. On day 22, media was aspirated, and Phase IV media (Table 16) was added, incubated at 37ºC, 5% CO_2 at a speed of 60rpm for 7 days. Cells were hemi-fed on day 26. On day 29, media was aspirated and Phase V media was dispensed (Table 17), incubated at 37ºC, 5% CO_2 at a speed of 60rpm for 7 days. Cells were then hemi-fed on day 31 and 34 and dissociated on day 36.

Neurospheres Dissociation

1ml of Neurospheres were harvested using a 10ml serological pipette. 2ml of Accutase was added to 1ml of spheres and sat for 10 minutes. Accutase was then removed and 2ml of papain containing DNase was added and incubated at 37°C for 30 minutes. Papain was removed and 1ml of EBSS, Ovomucoid and DNase mix was added and triturated Neurospheres 12 times using 1ml pipette. Triturated neurospheres were then filtered using a 0.7um cell strainer and spun for 3 minutes at 1500rpm. Supernatant was removed and 2ml of Phase V media was used to mix cells. Ovomucoid Inhibitor was carefully added on top of mixture and spun at 4000 rpm and resuspended in Phase V media. Cells were then ready to be plated.

Immunofluorescence Staining

Prior to platting cells, plates were coated with PDL then aspirated and rinsed twice with water and air-dried overnight in a biological safety cabinet. Afterwards, plates were incubated in Matrigel (Corning) overnight at 37^{o}C, 5% CO_2 to promote organization and growth. mDa cells were plated at a density of 12500 cells/well in Phase 5 medium, incubated at 37^{o}C, 5% CO_2 and hemi-fed every 2 days for 14 days. Cells were then fixed in 4% PFA, washed using PBS and blocked using blocking solution (3% normal goat serum + 0.3% triton/PBS). Wells were stained with TH and Beta-3 tubulin primary antibody at 4^{o}C overnight. After the wash with PBS, cells were stained with secondary antibody + Hoechst for 1 hour at RT, washed and imaged using Opera Phoenix high-content system.

RNA Purification

Cells harvested during each phase of mDA differentiation were frozen at -80^{o}C and used for RNA purification. Frozen cells were first purified to RNA using RNeasy Mini Kit from QIAGEN. During RNA purification, cells were mixed with 70% ethanol and Buffer RLT, triturated using a P1000 pipette and transferred to QIAshredder spin column and centrifuged to complete homogenization. Flow-through content was then placed in RNeasy Mini spin column and centrifuged, discarding flow-through. RNeasy Mini spin column was washed 3 times using RW1 and RPE buffers respectively. Once wash steps were completed, RNase-free water was added to spin column for elution, and flow-through collected.

Reverse Transcription

2ug of total RNA of each sample was used to generate cDNA. 20ul reaction mix was prepared using Thermofisher RNA-to-cDNA kit buffers. Reaction mixes were then incubated for 37^{o}C for 60 minutes. Reaction was then stopped by heating to 95^{o}C for 5 minutes and held at 4^{o}C. Generated cDNA was frozen at -20^{o}C until ready to use.

RT-PCR

The reaction was performed using TaqMan Gene Expression Master Mix 2x, GAPDH VIC probe, and genes of interest using FAM probe, creating a multiplex assay. The reaction was carried out using ViiA 7 Quant Studio System. On Table 18 shows the cycle information used for the RT-PCR. The levels of mRNA expression of analyzed genes were normalized to the housekeeping GAPDH to calculate ΔCt, follow by normalization

to Stem Cell group using the $2^{-\Delta\Delta Ct}$ method. Statistically significant differences were analyzed using One-way ANOVA.

MEA Assay

A 96-well CytoView MEA plate (Axion Biosystems) was coated with 80ul of 0.07% poly ethyleneimine (PEI) solution at 37ºC for 1 hour. PEI solution was then aspirated out and rinsed twice with water and air-dry overnight in a biological safety cabinet. Dissociated mDA neurons were suspended in Phase 5 media containing 10ug/ml of laminin, at a density of 100,000 cells per well. Plate was incubated at 37ºC, 5% CO_2 and hemi-fed every 2 days for a period of 20 days. MEA plate was recorded for 15 minutes using MaestroPro from Axion Biosystems on day 5, 9, 12, 15, 17 and 20. Neural Metric Tool software was used to analyze the generated data. Statistically significant differences were analyzed using One-way ANOVA.

Ca^{2+} Influx Assay

Plates were coated with PDL then aspirated and then rinsed twice with water and air-dried overnight in a biological safety cabinet. Afterwards, the plates were incubated in Matrigel (Corning) overnight at 37ºC, 5% CO_2. Cells were plated at a density of 12500 cells/well in Phase 5 medium, incubated at 37ºC, 5% CO_2 and hemi-fed every 2 days for 14 days. On day 14, cells were incubated with FLIPR Calcium 6 probe for 2 hours at 37ºC, 5% CO_2. Cells were then treated with 5uM Kainic acid, 50 uM Ibotenic acid, 5mM potassium chloride (KLC) and 250uM N-methyl-D-aspartate (NMDA) ligand. Ca^{2+} Influx was then measure using FDSS 7000EX instrument for a period of 10 minutes.

Chapter III.

Results

Gene Expression

To characterize and validate the ability of iPSC to differentiate into dopaminergic neurons, we first looked at the origins of cells by investigating the markers of the three germ layers and extraembryonic tissue (trophoblast) at all five phases of the differentiation process. Cells were collected during each phase of the iPSC differentiation steps and processed together. The embryonic layer markers were investigated at the mRNA level, by calculating the gene expression relative fold change normalized to stem cell profile. For the germ layer markers, we looked at HAND1 gene, a trophoblast marker. We also investigated transcription factor GBX2, a marker for the ectodermal layer. For the mesodermal layer marker, we selected transcription factor Brachyury (Faial, Tiago et al., 2015). Lastly, transcription factor SOX17 was selected as the marker to represent the endodermal layer. In figure 2, we observe an increase in gene expression level at all phases for HAND1, with the highest expression level seen in Phase II with a 7.0-fold increase relative to Phase I. In figure 3, GBX2 had an increase in gene expression in Phase I and Phase II, declining as the phases transition progressed. For the mesodermal germ layer in figure 4, Brachyury expression was present during Phase I and Phase II. However, no expression levels were observed during Phase III, IV and V, as dopaminergic neurons began forming. Much like HAND1, SOX17 relative fold change peaked at Phase II, with a 3-fold increase, reducing fold change in subsequent phases (figure 5).

To further characterize the iPSC cells, next we looked at dopaminergic neuron transcription factor markers. First, we look at two important signaling molecules that is

implicated in the formation of dopaminergic neurons in the neural tube, SHH and FGF8 (Ye, W et al., 1998). SHH demonstrated to be highly expressed in all differentiation phases, peaking at Phase IV when cells are becoming more differentiated into mature dopaminergic neurons (Figure 6). FGF8 peaked at the early stages of differentiation, with a 2-fold increase from Phase I to Phase II, decreasing expression level as differentiation continued (Figure 7). We then looked at neuron progenitor's floor plate FOXA2 and roof plate LMX1A. FOXA2 had a high expression levels the early stages of the differentiation, during Phase I and II (Figure 8). LMX1A, on the other hand, showed highest expression level during Phase II and Phase IV (Figure 9). Lastly, we looked at dopaminergic post mitotic transcription factors. NURR1 is a transcription factor responsible for the maturation of dopaminergic neurons (Rodríguez-Traver, Eva et al., 2016). We observed that NURR1 relative fold change peaked at the two last stages of differentiation, with a 14.1-fold increase on Phase IV and 11.6-fold increase on Phase V relative to stem cell stage (Figure 10). To analyze whether the stem cells we used were maturing into neurons, we looked at neuronal marker TUBB. TUBB levels showed a gradual increase in gene expression as the differentiation stages progressed, with the highest expression level observed during Phase IV and Phase V (Figure 11). Lastly, we analyzed dopaminergic neuron marker TH. Similar to TUBB, TH is highly expressed, and its expression level progressively increased as the differentiation progressed, peaking at the last phase (Figure 12).

Calcium imaging

Bound calcium probe cells were treated with KCL, NMDA ligand and excitotoxic compounds Kainic acid and Ibotenic acid on day 14 post cell plating. Calcium fluorescence intensity was measured to calculate Calcium levels. TH marker was used to determine

excitotoxicity of Kainic acid and Ibotenic acid. DMSO group showed no calcium influx as expected (Figure 17). Once cells were treated with KLC, there was an increase in Ca^{2+} probe dye ratio, with the max fluorescence ratio peak reaching 1.86 (Figure 13). NMDA treated cells had an increase of Ca^{2+} probe dye ratio, with the max fluorescence ratio reaching 1.79 (Figure 14). Compound Ibotenic acid also showed an increase in calcium levels, its max fluorescence ratio reaching 1.82 (Figure 15), and a 3.0-fold decrease in TH positive cell population (Figure 18). Similarly, excitotoxic compound Kainic acid, showed an increase of Ca^{2+} probe dye ratio, with the highest max fluorescence ratio of all treated cells of 1.91 (Figure 16) and 3.0-fold decrease in TH positive cells (Figure 19).

MEA Assay

Spontaneous neuronal activity was acquired at 37ºC, 5% CO_2 using a MEA system. The mean firing rate on day 5 was as low as 0.002 Hz (Figure 20) and 1.8 spikes burst (Figure 21), registering a low neuronal activity on the first read out. On the subsequent days, we observed a gradual increase in mean firing rate on over time, from 0.04 Hz at day 9, to 2.4 Hz on day 20. We also observed a significant increase in the number of spikes, from 38 spikes on day 9, to 2196 spikes on day 20.

Chapter IV.

Discussion

PD is an incurable disease and one of the biggest unmet medical in modern society. There is a need to generate dopaminergic neurons in vitro, to better study the pathological conditions underlying the dopaminergic neuron degeneration observed in the disease. The purpose of this study was to generate iPSC-derived dopaminergic neurons that expresses classical biochemical traits and show neuronal excitability and transmission. Generating a robust protocol, will guarantee a high efficiency, standardization, and reproducible data.

In the first set of experiments, we analyzed the early stages of iPSC stem cell differentiation and their capabilities to differentiate into neurons and dopaminergic neurons. Through gene expression analysis we looked at several markers at all five phases of the differentiation process. To begin our iPSC characterization, we first analyzed the germ layers whose induction is responsible for forming various kinds of somatic cells. HAND1 is an important transcription factor for the development of the trophoblast, which is essential for the formation of the placenta (Scott, I C et al., 2000). Here, we observed statistically significant difference in levels of HAND1, which had a 30-fold increase in gene expression relative to Stem cell during Phase II of differentiation. However, HAND1 expression level decreased as expected, as cells became more differentiated into neurons. We also analyzed the ectoderm germ layer, which is responsible in the formation of the central nervous system, by looking at transcription factor GBX2 (Liu A et al., 2001). GBX2 expression level increased in the early stages on the differentiation, during Phase I and Phase II, decreasing in subsequent phases. A conclusion could not be reached as to why GBX2 levels decreased from Phase III-V, further experiments will need to be done to

understand results. For the mesoderm layer, which gives rise to muscle cells and connective tissues, we selected transcription factor Brachyury. Brachyury was only expressed during Phase I and II, with a low expression relative to stem cell stage, which is expected as the late stages are related to neurons and not muscle cells or connective tissues. The last germal layer we analyzed was the endoderm (transcription factor SOX17), which gives rise to organs such as the stomach and intestines (Séguin, Cheryle A et al., 2008). Much like HAND1, SOX17 had the highest expression level during phase II, and had a low expression in the subsequent phases.

To better understand the process of differentiation to dopaminergic neurons, we looked at markers present at different stages of dopaminergic neurons formation. SHH is an important signaling molecule in the formation of the neural tube, the embryonic precursor to the central nervous system (Hynes, M et al., 1995). SHH is also crucial in the formation of motor neurons. As such, SHH was highly expressed at all phases of the differentiation, ranging from 100 to 400-fold change relative to stem cell expression, as was expected.

Next, we looked at neural progenitor markers LMX1A and FOXA2. FOXA2 is a floor plate marker that regulates dopaminergic neurons generation and differentiation (Arenas, Ernest et al., 2008). LMX1A is a roof plate marker which is important in the development of dopaminergic neurons and survival of adult dopaminergic neurons (Doucet-Beaupré, Hélène et al., 2016). We observed that both progenitor markers were highly expressed at all differentiation phases. FOXA2 had a 50-fold relative expression increase at the early phases (Phase I and II). Interestingly, LMX1A reached a 300-fold

increase in relative expression levels at Phase II and IV, which correlates with the marker being important in the early and late stages of dopaminergic neuron development.

We then looked at post-mitotic dopaminergic transcription factor NURR1. NURR1 is an important transcription factor for the maturation of dopaminergic neurons, their mutation is associated with the human disease PD (Rodríguez-Traver, Eva et al., 2016). Here we observed a gradual increase in expression levels from Phase I-III, then we detected a 14.1-fold increase on Phase IV, and 11.6-fold increase in relative expression at Phase V. The peak expression level in the last two differentiation phases, compared to the early phases, correlates with NURR1 being important for the maturation of dopaminergic neurons.

To confirm whether the iPSC's cells are being differentiated into neuronal cells, and more importantly into dopaminergic neurons, we looked at neuronal marker TUBB and dopaminergic neuron marker TH. Both markers were highly expressed in all phases. TH on Phase I had a 28.5-fold expression increase relative to stem cell stage, progressively increasing as cells were maturing into dopaminergic neurons, reaching a 5058.0-fold increase in expression level on Phase V. Similarly, TUBB gradually increased in expression levels as differentiation phases progressed. Both markers were also observed in fluorescence imaging, demonstrating once iPSC's cells matured they developed into dopaminergic neurons (Figure 1).

We can conclude that iPSC cells expressed early neuronal progenitor transcription factors during the early stages while dopaminergic neurons were forming, and progressively matured into dopaminergic neurons as indicated by the highly expressed NURR1 and TH markers.

To characterize the dopaminergic neurons from a functional angle, we performed electrophysiological recording of signals from neuronal cultures plated using multi electrode array assay. Neurons requires to be cultured for several days to mature so axons and dendrites can form, and active synapses transmission can occur between cells. On day 5, we observed minimal neuronal activity, with a mean firing rate of 0.002 Hz and 1.8 spikes burst, which demonstrates the cells were not matured enough to show neuronal functionality. As cells matured, we observed a significant increase in mean firing rate and spikes over time, reaching a max mean firing rate of 2.4 Hz and 2196 spikes on day 20. This confirms our dopaminergic neurons are spontaneously firing action potentials frequently, which is an indication of neuronal functionality.

While MEA's looks at activity of the cells, calcium influx regulates the neurotransmitter release, which correlates with action potential (Thanawala et al., 2013). On our last aim to characterize our iPSC's, we looked at calcium influx. We used calcium labeled molecules that exhibited an increase in fluorescence upon binding Ca^{2+} to measure Ca^{2+} influx. Ca^{2+} are important messengers which tells pre-synaptic axon terminals to release neurotransmitters as a form of synapse. Interfering with Ca^{2+} by increasing its levels can lead to neuronal death (Gleichmann, Marc et al., 2010). We were able to assess Ca^{2+} levels in our dopaminergic neurons in the presence or absence of the compound. In other to determine whether the dopaminergic neurons were functional or not, in our first experiment we depolarized the membrane of our dopaminergic neurons using KCL. KCL increases the concentration of potassium gradient outside of the cell, which makes potassium want to achieve equilibrium by pumping potassium from inside the cell – outside of the cell. Consequently, to reach equilibrium sodium gradient will be pumped from its

high concentration from outside – inside the cell, resulting in the depolarization of the cell (Rienecker et al., 2020). Here, we were able to observe this phenomenon with a rapid increase in Ca^{2+} probe dye ratio in KCL treated cells, which indicated an increase in intracellular Ca^{2+} influx in the dopaminergic neurons. This demonstrated the depolarization of the presynaptic terminal caused the voltage gated calcium channel to open, allowing the influx of Ca^{2+} into the cell, which signaled the release of neurotransmitters.

NMDA receptors are an important regulator of dopaminergic neurons activity (Bonci et al., 1999), thus next, the expression of functional ligand-gated ion channel NMDA was examined. We treated cells with NMDA ligand and NMDA agonist Ibotenic acid. Here we observed a rapid increase of Ca^{2+} probe dye ratio from baseline in both ligand and agonist as expected. These results indicate that the iPSC-derived dopaminergic neurons express functional NMDA receptors.

Lastly, we treated cells with AMPA agonist Kainic acid, a compound known to induce PD due to its excitotoxicity capabilities, which causes an accumulation of Ca^{2+} seen *in vivo* (Foster et al., 2003). Consistently with the other compounds, we observed a rapid increase in Ca^{2+} probe dye ratio as well, displaying the highest max ratio of all treated cells. This correlates with what was seen in Foster et al *in vivo* study.

Due to Ibotenic acid and Kainic acid excitotoxicity capabilities in dopaminergic neurons, these two compounds demonstrated to induce a progressive death of substantia nigra neurons *in vivo* (Foster et al., 2003, Pasinetti et al., 1991). Here, we were able to observe a 3.0-fold decline in TH positive cells relative to DMSO group for both Ibotenic acid and Kainic acid treated cells. This result reflected the neurodegeneration abilities by both excitotoxic compounds.

Taken together the results from all the experiment we report here, show we can efficiently differentiate human iPSCs in mature and active dopaminergic neurons and this model may be potentially used for further investigation of therapies against PD.

Appendix I.

Definition of Terms

"A53T": A point mutation of the α-syn protein, which results in the formation of aggregate proteins

"AMPA": is an ionotropic transmembrane receptor for glutamate

"Autophagy": A mechanism by which the cells in our body degrade unnecessary or damaged components within the cell

"α-synuclein (α-syn)": An abundant protein, whose aggregate misfolded form is one of the leading causes of PD

"ATP13A2": A gene which encodes for lysosomal ATPase

"ATPase": A pump that is involved in cation and polyamine transport, the polyamine-transporting ATPase 13A

"β-glucocerebrosidase (GCase)": A lysosomal enzyme that hydrolyses glucosylceramide to ceramide and glucose

"Biochemical models": Models used to study the binding or activity of a biological molecule

"Bradykinesia": Slowness of movements

"Cellular models": Models that represent the actual cellular environment, acting as an intermediate between biochemical screens and the capacity to predict in vivo effects

"Electrode treatment": Deep brain stimulation through surgically implanting an electrode

"FOXA2": Forkhead family of winged-helix transcription factor 2

"GBX2": Gastrulation brain homeobox 2

“Dopaminergic neurons”: Found in the substantial nigra region of the brain and play an essential role in the control of voluntary motor movement

“GBA”: A gene that encodes for lysosomal enzyme β-glucocerebrosidase (GCase)

“HAND1”: Heart and neural crest derivatives expressed 1

“Ibotenic Acid”: NMDA agonist

“Immortalized cells”: Cells that can grow indefinitely

“Induced Pluripotent Stem Cell (iPSC)”: Derived from skin or blood cells that have been reprogrammed back into an embryonic-like pluripotent state, enabling the development of an unlimited source of any type of human cell needed for therapeutic purposes

“In vitro”: Designed with components of cells that have been isolated to monitor biochemical and functional reactions to determine mechanism of actions and impact of novel therapeutics.

“In vivo”: Experiments and procedures that researchers perform in or on a whole living organism

“Kainic Acid”: AMPA agonist

“Potassium chloride”: cell depolarization inducer

“Lewy-bodies”: Inclusions that are typically found in PD patients. They contain aggregate misfolded α-syn proteins, lipids and organelle fragments

“LMX1A”: LIM homeobox transcription factor 1 alpha

“Lysosome”: organelles involved in the degradation of intracellular and extracellular macromolecules

“MEA”: Multielectrode Array

“Mechanism of action (MOA)”: Refers to the specific biochemical interaction through which a drug substance produces its pharmacological effect

“Mitophagy”: The removal of defective mitochondria following damage or stress by specialized autophagy

“Mitochondria”: Membrane-bound cell organelles that generate most of the chemical energy needed to power the cell's biochemical reactions

“Neurodegenerative disorder”: A type of disease in which cells of the central nervous system stop working or die

“NMDA”: Ionotropic glutamate receptors

“NURR1”: Orphan nuclear receptor

“PARKIN”: Is the gene that encodes for Parkin protein, responsible for the activation of mitophagy

“Parkinson Disease (PD)”: A neurodegenerative disorder that affects predominately dopamine-producing (“dopaminergic”) neurons

“PINK1”: The gene that encodes for PTEN-induced kinase 1 (PINK1), a kinase upstream of PARKIN, which phosphorylates PARKIN protein to induce mitophagy

“Primary cellular model”: Cellular models that are taken directly from the tissue through enzymatic or mechanical measures and optimized under culture conditions

“Reactive oxygen species (ROS)”: Serve as cell signaling molecules for normal biologic processes. However, the generation of ROS can also provoke damage to multiple cellular organelles and processes.

“SNCA”: Gene that encodes for α-syn

“SOX17”: SRY-box transcription factor 17

“TH”: Tyrosine Hydroxylase, a dopaminergic neuron marker

“TOMM20”: Translocase of Outer Mitochondrial Membrane 20

“TUBB”: Beta-III-tubulin, a neuronal marker

Appendix II.

Figures and Tables

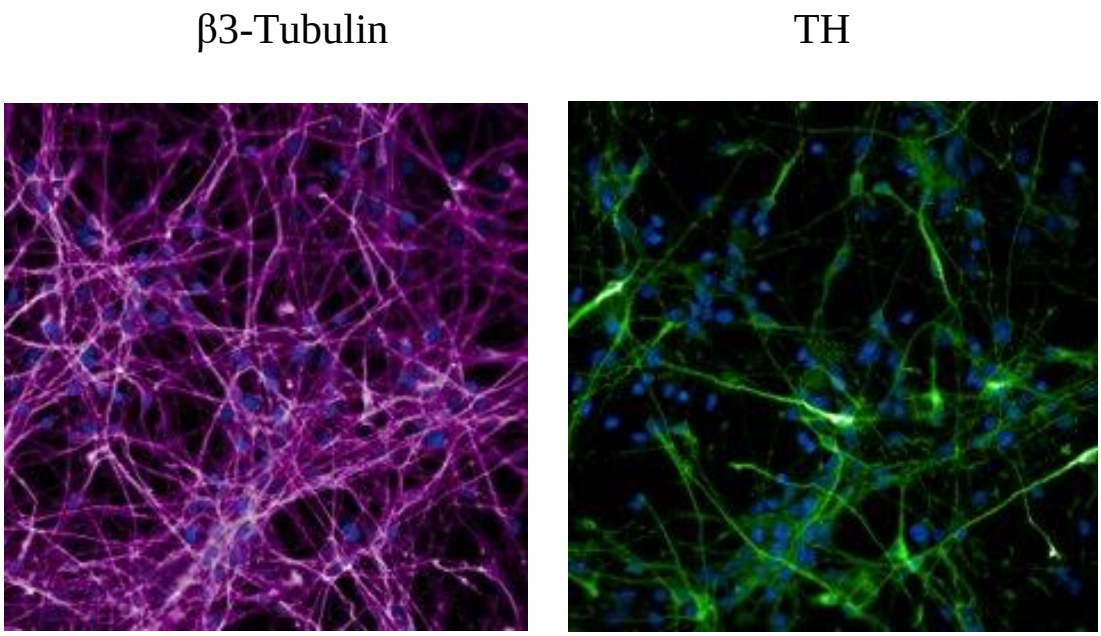

Figure 1. Matured iPSC-derived Dopaminergic Neuron

Representative fluorescence images of dopaminergic neuron marker TH (green), neuronal marker β3-tubulin (purple), and nucleus Hoechst (blue). Phase V cells were dissociated, plated, incubated at 37°C, 5% CO_2 and hemi-fed every 2 days for 14 days. Cells were then fixed with 4% PFA, and stained. Imaged was taken using Opera Phoenix high-content system.

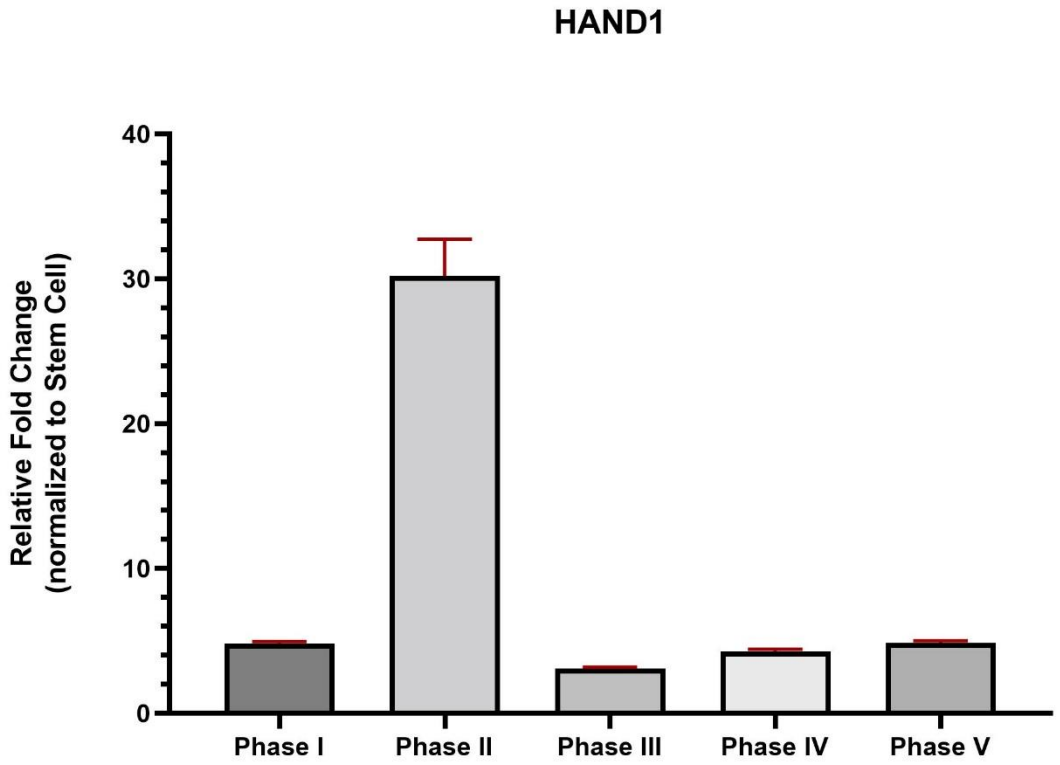

Figure 2. HAND1 Gene Expression

*Graph representing mRNA expression level of trophoblast marker HAND1. Relative expression of genes was calculated by RT-qPCR with the ΔΔCt method, using GAPDH as a constitutive control, and normalizing the differentiation phases to Stem cell stage to calculate relative fold change, n= 3. No statistical significance differences were observed between Phase IV and Phase V. The data represent the mean ± SEM. n.s not significant, ****: p<0.0001 as assessed by One-way ANOVA.*

Table 1. Ordinary one-way ANOVA multiple comparison HAND1 Gene Expression

Tukey's multiple comparisons test	Summary	Adjusted P Value
Phase I vs. Phase II	****	<0.0001
Phase I vs. Phase III	ns	0.819
Phase I vs. Phase IV	ns	0.9964
Phase I vs. Phase V	ns	>0.9999
Phase II vs. Phase III	****	<0.0001
Phase II vs. Phase IV	****	<0.0001
Phase II vs. Phase V	****	<0.0001
Phase III vs. Phase IV	ns	0.9485
Phase III vs. Phase V	ns	0.806
Phase IV vs. Phase V	ns	0.9953

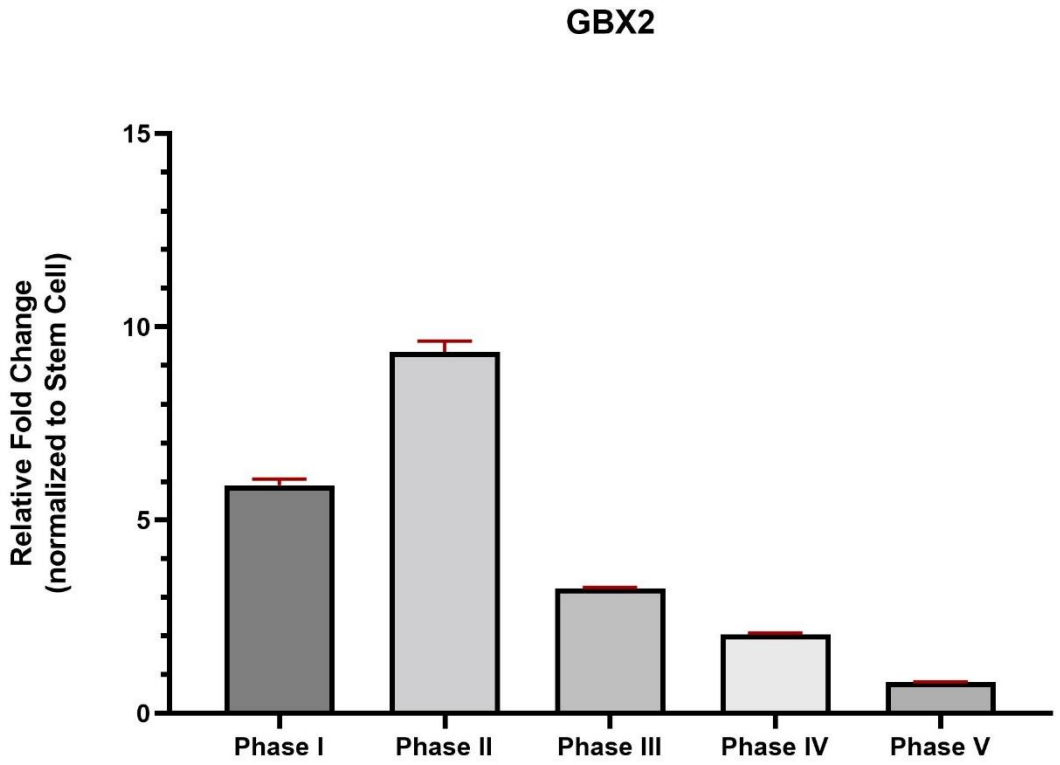

Figure 3. GBX2 Gene Expression

*Graph representing mRNA expression level of ectodermal germ layer marker GBX2. Relative expression of genes was calculated by RT-qPCR with the ΔΔCt method, using GAPDH as a constitutive control, and normalizing the differentiation phases to Stem cell stage to calculate relative fold change, n= 3. The data represent the mean ± SEM. *: n.s not significant, ***: p<0.0003, ****: p<0.0001 as assessed by One-way ANOVA.*

.

Table 2. Ordinary one-way ANOVA multiple comparison GBX2 Gene Expression

Tukey's multiple comparisons test	**Summary**	**Adjusted P Value**
Phase I vs. Phase II	****	<0.0001
Phase I vs. Phase III	****	<0.0001
Phase I vs. Phase IV	****	<0.0001
Phase I vs. Phase V	****	<0.0001
Phase II vs. Phase III	****	<0.0001
Phase II vs. Phase IV	****	<0.0001
Phase II vs. Phase V	****	<0.0001
Phase III vs. Phase IV	***	0.0003
Phase III vs. Phase V	****	<0.0001
Phase IV vs. Phase V	***	0.0002

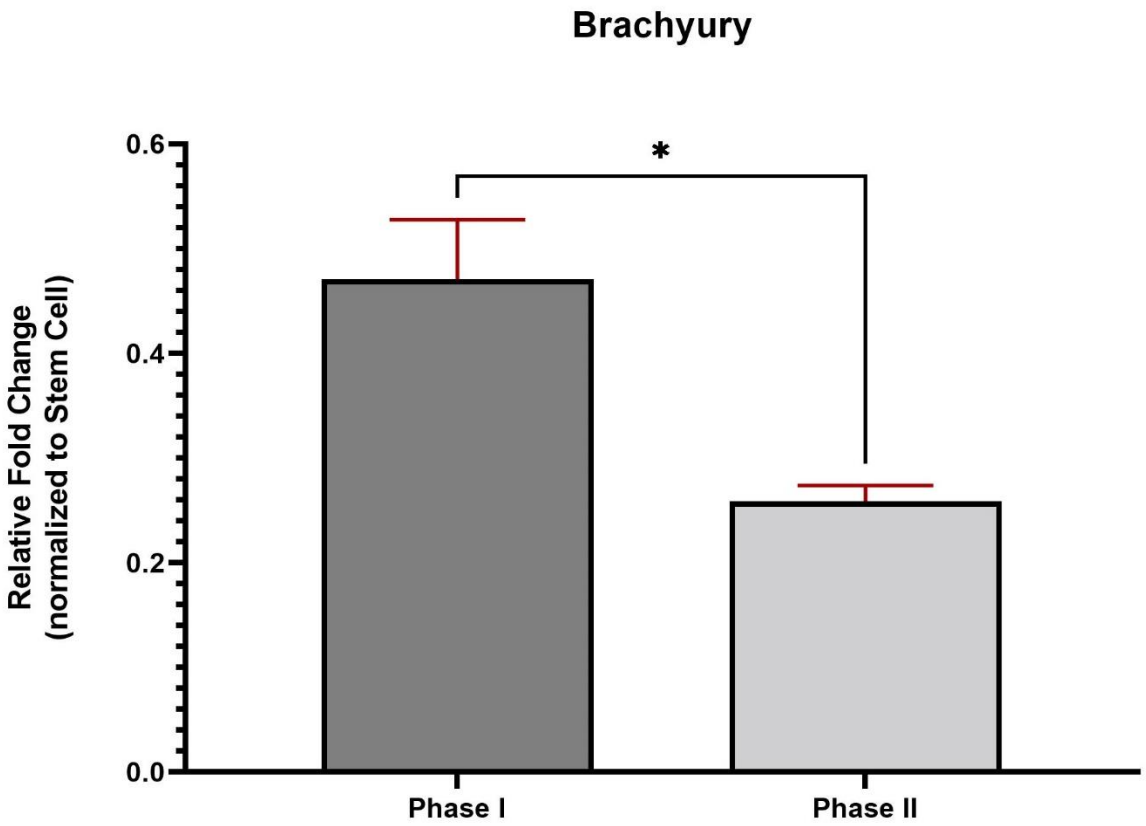

Figure 4. Brachyury Gene Expression

*Graph representing mRNA expression level of mesodermal germ layer marker Brachyury. Relative expression of genes was calculated by RT-qPCR with the ΔΔCt method, using GAPDH as a constitutive control, and normalizing the differentiation phases to Stem cell stage to calculate relative fold change, n= 3. No expression level was observed in Phase III-V. The data represent the mean ± SEM. *: p<0.05 as assessed by one tailed Student's T test.*

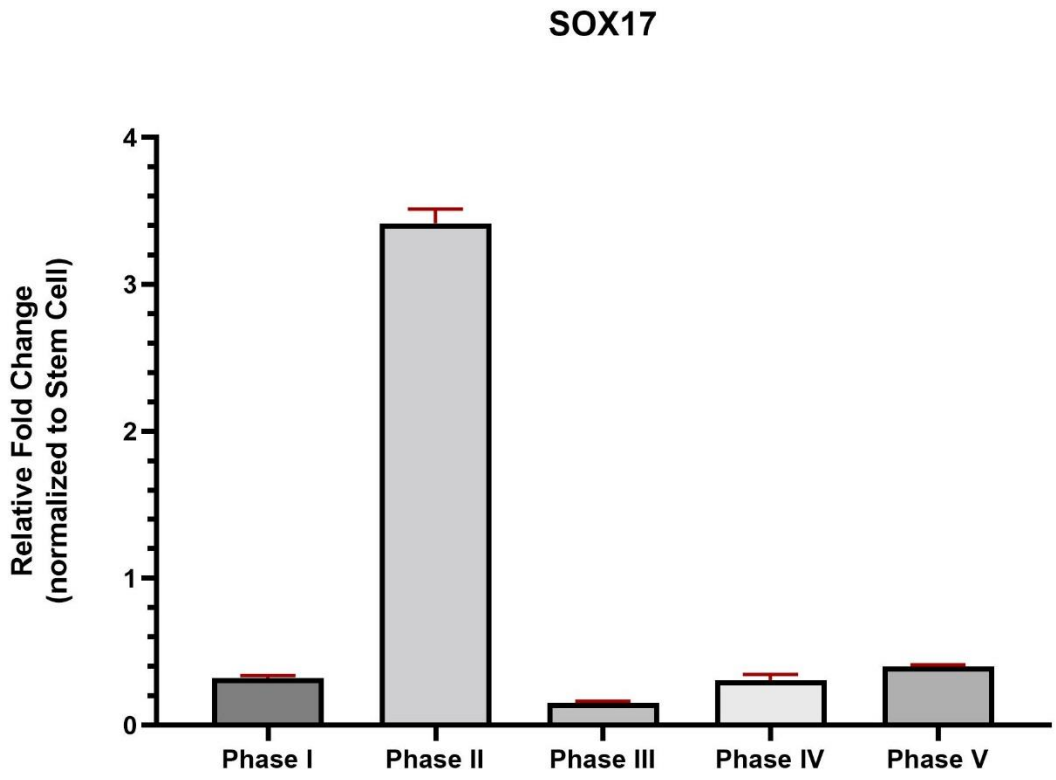

Figure 5. SOX17 Gene Expression

*Graph representing mRNA expression level of endodermal germ layer marker SOX17. Relative expression of genes was calculated by RT-qPCR with the ΔΔCt method, using GAPDH as a constitutive control, and normalizing the differentiation phases to Stem cell stage to calculate relative fold change, n= 3. No statistical significance differences were observed between Phase IV and Phase V. The data represent the mean ± SEM. n.s not significant, *: p<0.02, ****: p<0.0001 as assessed by One-way ANOVA.*

Table 3. Ordinary one-way ANOVA multiple comparison SOX17 Gene Expression

Tukey's multiple comparisons test	Summary	Adjusted P Value
Phase I vs. Phase II	****	<0.0001
Phase I vs. Phase III	ns	0.1423
Phase I vs. Phase IV	ns	0.9997
Phase I vs. Phase V	ns	0.7460
Phase II vs. Phase III	****	<0.0001
Phase II vs. Phase IV	****	<0.0001
Phase II vs. Phase V	****	<0.0001
Phase III vs. Phase IV	ns	0.1940
Phase III vs. Phase V	*	0.0152
Phase IV vs. Phase V	ns	0.6378

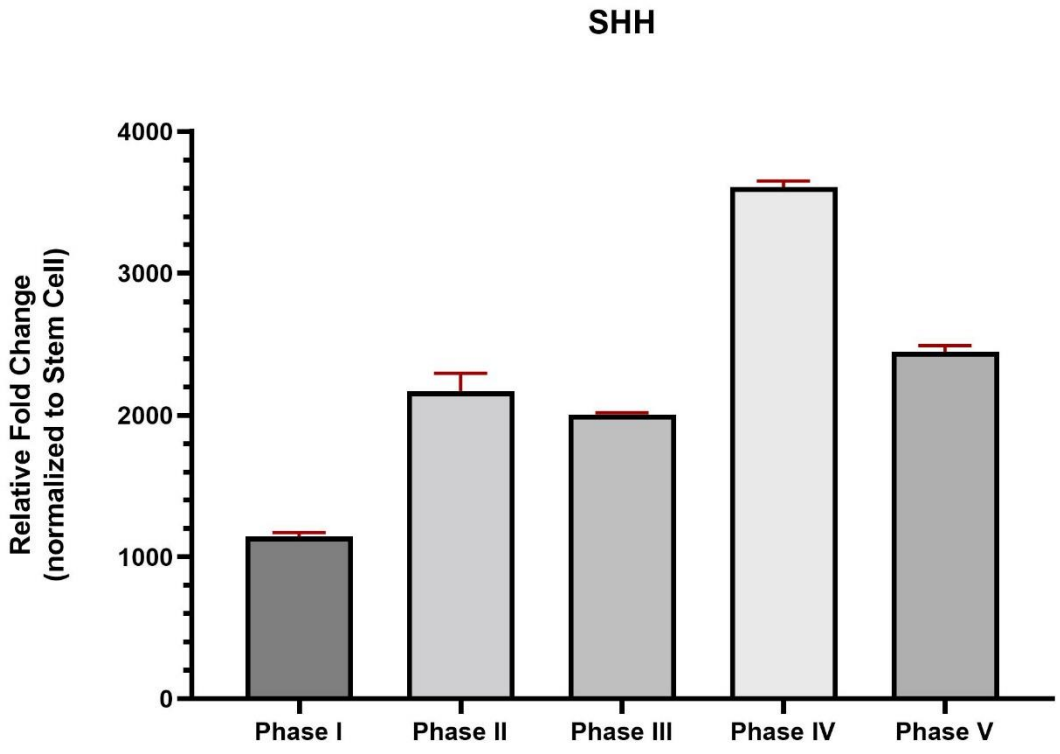

Figure 6. SHH Gene Expression

*Graph representing mRNA expression level of signaling molecule marker SHH. Relative expression of genes was calculated by RT-qPCR with the ΔΔCt method, using GAPDH as a constitutive control, and normalizing the differentiation phases to Stem cell stage to calculate relative fold change, n= 3. No statistical significance differences were observed between Phase II and Phase III. The data represent the mean ± SEM. n.s not significant, **: p<0.002, ****: p<0.0001 as assessed by One-way ANOVA.*

Table 4. Ordinary one-way ANOVA multiple comparison SHH Gene Expression

Tukey's multiple comparisons test	Summary	Adjusted P Value
Phase I vs. Phase II	****	<0.0001
Phase I vs. Phase III	****	<0.0001
Phase I vs. Phase IV	****	<0.0001
Phase I vs. Phase V	****	<0.0001
Phase II vs. Phase III	ns	0.4009
Phase II vs. Phase IV	****	<0.0001
Phase II vs. Phase V	ns	0.0524
Phase III vs. Phase IV	****	<0.0001
Phase III vs. Phase V	**	0.0016
Phase IV vs. Phase V	****	<0.0001

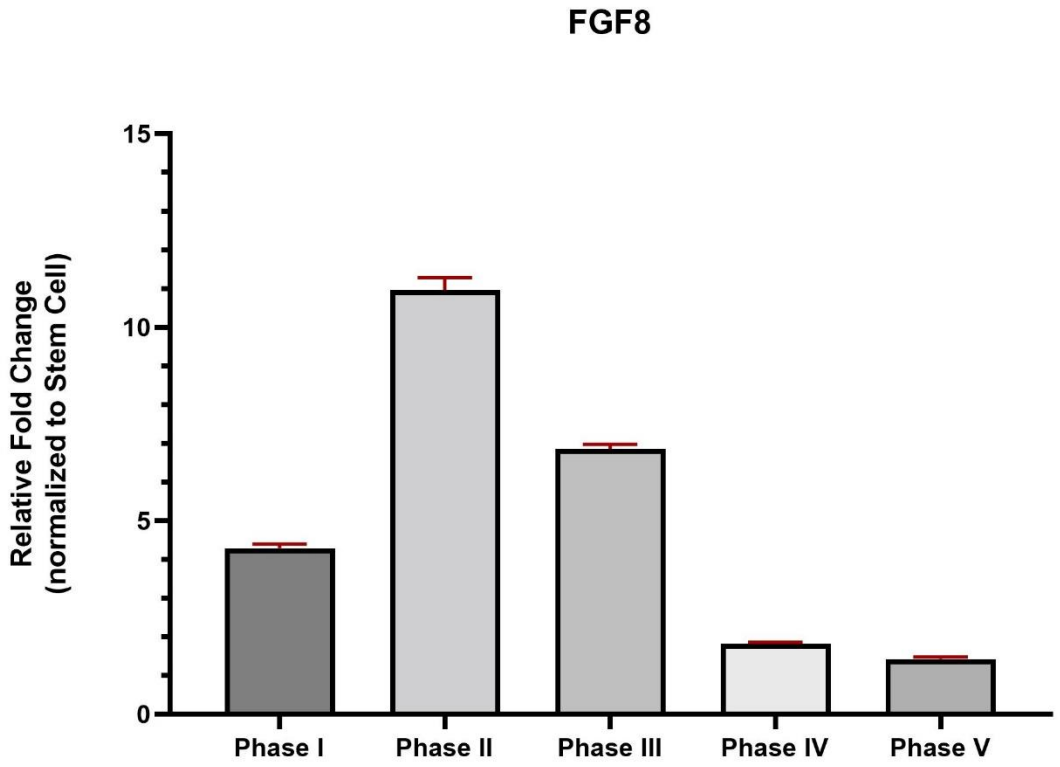

Figure 7. FGF8 Gene Expression

*Graph representing mRNA expression level of signaling molecule marker FGF8. Relative expression of genes was calculated by RT-qPCR with the ΔΔCt method, using GAPDH as a constitutive control, and normalizing the differentiation phases to Stem cell stage to calculate relative fold change, n= 3. The data represent the mean ± SEM. *: n.s not significant, ****: p<0.0001 as assessed by One-way ANOVA.*

Table 5. Ordinary one-way ANOVA multiple comparison FGF8 Gene Expression

Tukey's multiple comparisons test	Summary	Adjusted P Value
Phase I vs. Phase II	****	<0.0001
Phase I vs. Phase III	****	<0.0001
Phase I vs. Phase IV	****	<0.0001
Phase I vs. Phase V	****	<0.0001
Phase II vs. Phase III	****	<0.0001
Phase II vs. Phase IV	****	<0.0001
Phase II vs. Phase V	****	<0.0001
Phase III vs. Phase IV	****	<0.0001
Phase III vs. Phase V	****	<0.0001
Phase IV vs. Phase V	ns	0.4847

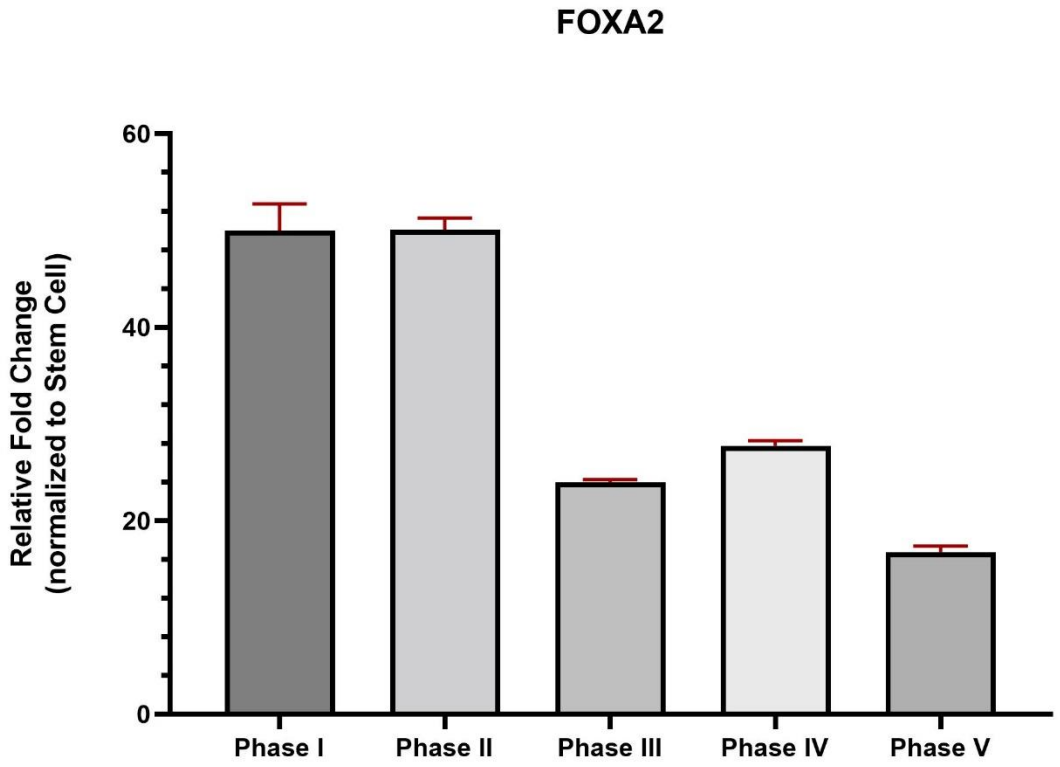

Figure 8. FOXA2 Gene Expression

*Graph representing mRNA expression level of neuron early progenitor floor plate LMX1A. Relative expression of genes was calculated by RT-qPCR with the ΔΔCt method, using GAPDH as a constitutive control, and normalizing the differentiation phases to Stem cell stage to calculate relative fold change, n= 3. No statistical significance differences were observed between Phase I and Phase II. The data represent the mean ± SEM. n.s not significant, *: p<0.02, ***: p<0.0005, ****: p<0.0001 as assessed by One-way ANOVA.*

Table 6. Ordinary one-way ANOVA multiple comparison FOXA2 Gene Expression

Tukey's multiple comparisons test	Summary	Adjusted P Value
Phase I vs. Phase II	ns	>0.9999
Phase I vs. Phase III	****	<0.0001
Phase I vs. Phase IV	****	<0.0001
Phase I vs. Phase V	****	<0.0001
Phase II vs. Phase III	****	<0.0001
Phase II vs. Phase IV	****	<0.0001
Phase II vs. Phase V	****	<0.0001
Phase III vs. Phase IV	ns	0.3484
Phase III vs. Phase V	*	0.0176
Phase IV vs. Phase V	***	0.0005

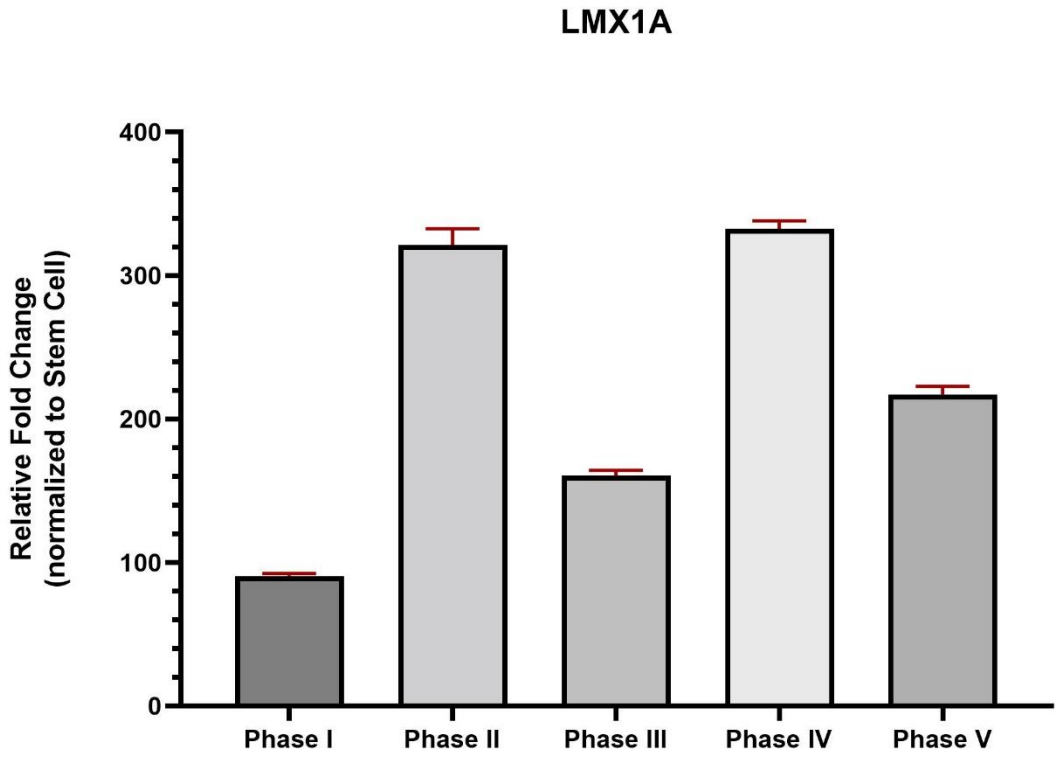

Figure 9. LMX1A Gene Expression

*Graph representing mRNA expression level of neuron early progenitor roof plate LMX1A. Relative expression of genes was calculated by RT-qPCR with the ΔΔCt method, using GAPDH as a constitutive control, and normalizing the differentiation phases to Stem cell stage to calculate relative fold change, n= 3. The data represent the mean ± SEM. n.s not significant, ***: p<0.0002, ****: p<0.0001 as assessed by One-way ANOVA.*

Table 7. Ordinary one-way ANOVA multiple comparison LMX1A Gene Expression

Tukey's multiple comparisons test	Summary	Adjusted P Value
Phase I vs. Phase II	****	<0.0001
Phase I vs. Phase III	****	<0.0001
Phase I vs. Phase IV	****	<0.0001
Phase I vs. Phase V	****	<0.0001
Phase II vs. Phase III	****	<0.0001
Phase II vs. Phase IV	ns	0.7272
Phase II vs. Phase V	****	<0.0001
Phase III vs. Phase IV	****	<0.0001
Phase III vs. Phase V	***	0.0002
Phase IV vs. Phase V	****	<0.0001

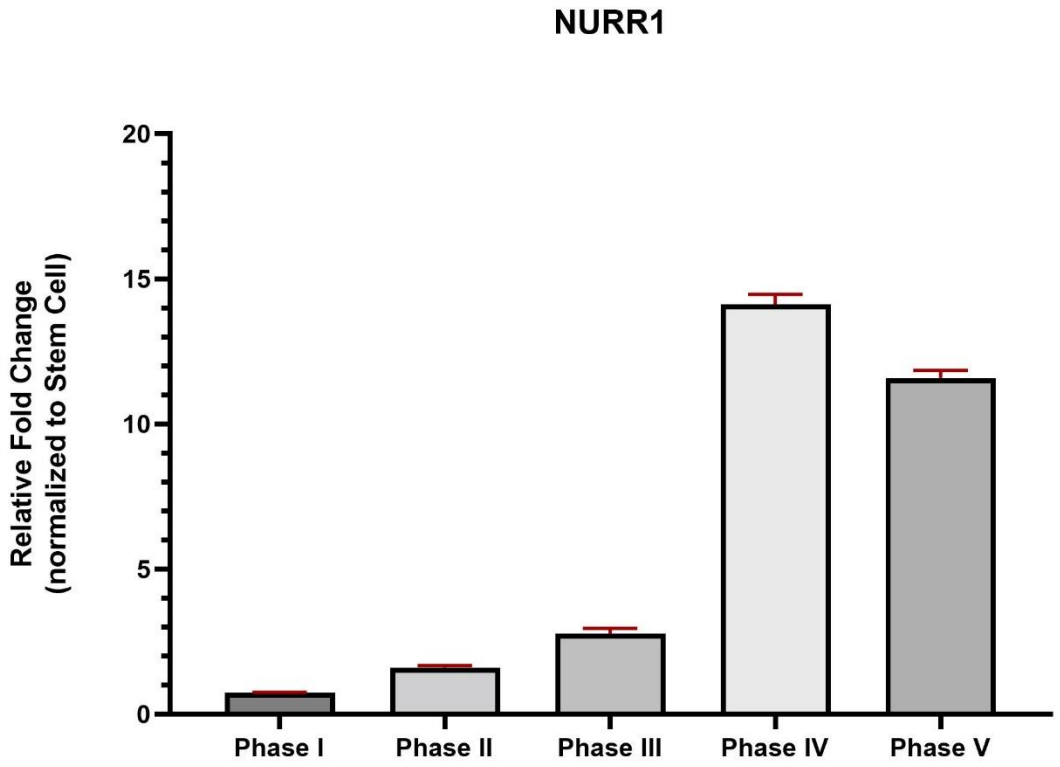

Figure 10. NURR1 Gene Expression

*Graph representing mRNA expression level of transcription factor responsible for the maturation of dopaminergic neurons NURR1. Relative expression of genes was calculated by RT-qPCR with the ΔΔCt method, using GAPDH as a constitutive control, and normalizing the differentiation phases to Stem cell stage to calculate relative fold change, n= 3. The data represent the mean ± SEM. n.s not significant, *: p<0.02, ****: p<0.0001 as assessed by One-way ANOVA.*

Table 8. Ordinary one-way ANOVA multiple comparison NURR1 Gene Expression

Tukey's multiple comparisons test	Summary	Adjusted P Value
Phase I vs. Phase II	ns	0.0791
Phase I vs. Phase III	****	<0.0001
Phase I vs. Phase IV	****	<0.0001
Phase I vs. Phase V	****	<0.0001
Phase II vs. Phase III	*	0.0132
Phase II vs. Phase IV	****	<0.0001
Phase II vs. Phase V	****	<0.0001
Phase III vs. Phase IV	****	<0.0001
Phase III vs. Phase V	****	<0.0001
Phase IV vs. Phase V	****	<0.0001

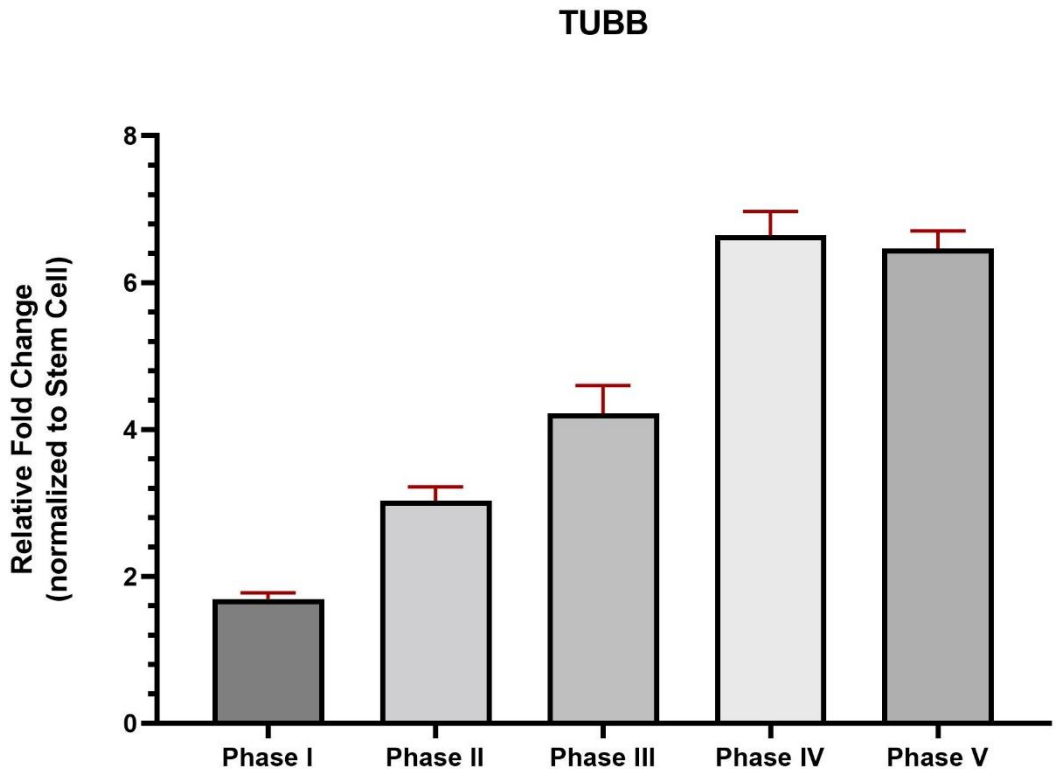

Figure 11. TUBB Gene Expression

*Graph representing mRNA expression level of neuronal marker TUBB. Relative expression of genes was calculated by RT-qPCR with the ΔΔCt method, using GAPDH as a constitutive control, and normalizing the differentiation phases to Stem cell stage to calculate relative fold change, n= 3. No statistical significance differences were observed between Phase II – III, and Phase IV – V. The data represent the mean ± SEM. n.s not significant, *: p<0.02, ***: p<0.0002, ****: p<0.0001 as assessed by One-way ANOVA.*

Table 9. Ordinary one-way ANOVA multiple comparison TUBB Gene Expression

Tukey's multiple comparisons test	Summary	Adjusted P Value
Phase I vs. Phase II	*	0.0195
Phase I vs. Phase III	****	<0.0001
Phase I vs. Phase IV	****	<0.0001
Phase I vs. Phase V	****	<0.0001
Phase II vs. Phase III	*	0.0401
Phase II vs. Phase IV	****	<0.0001
Phase II vs. Phase V	****	<0.0001
Phase III vs. Phase IV	****	<0.0001
Phase III vs. Phase V	***	0.0002
Phase IV vs. Phase V	ns	0.9879

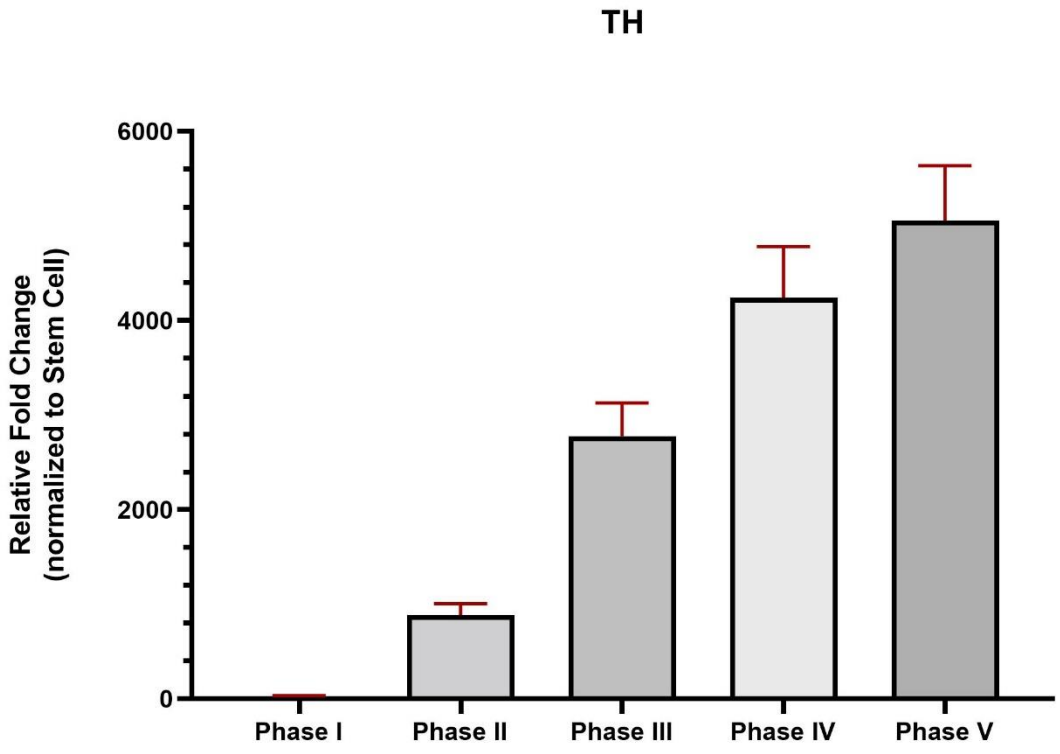

Figure 12. TH Gene Expression

*Graph representing mRNA expression level of dopaminergic neuron marker TH. Relative expression of genes was calculated by RT-qPCR with the ΔΔCt method, using GAPDH as a constitutive control, and normalizing the differentiation phases to Stem cell stage to calculate relative fold change, n= 3. No statistical significance differences were observed between Phase III – IV, and Phase IV – V. The data represent the mean ± SEM. n.s not significant, *: p<0.03, **: p<0.002, ***: p<0.0002, ****: p<0.0001 as assessed by One-way ANOVA*

Table 10. Ordinary one-way ANOVA multiple comparison TUBB Gene Expression

Tukey's multiple comparisons test	Summary	Adjusted P Value
Phase I vs. Phase II	ns	0.5493
Phase I vs. Phase III	**	0.0013
Phase I vs. Phase IV	****	<0.0001
Phase I vs. Phase V	****	<0.0001
Phase II vs. Phase III	*	0.0265
Phase II vs. Phase IV	***	0.0002
Phase II vs. Phase V	****	<0.0001
Phase III vs. Phase IV	ns	0.1106
Phase III vs. Phase V	**	0.0069
Phase IV vs. Phase V	ns	0.5931

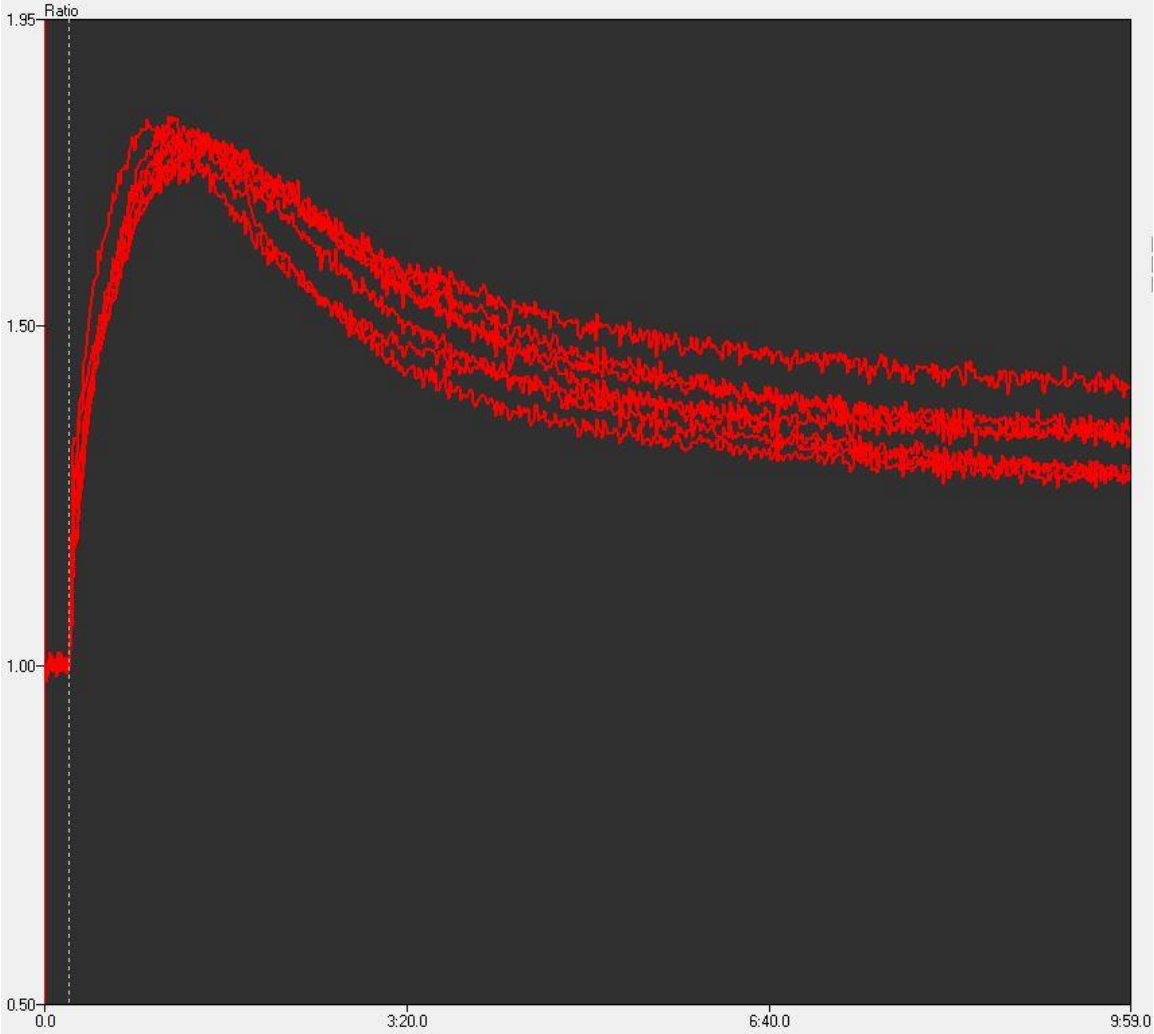

Figure 13. Potassium chloride Ca^{2+} influx

Graph representing Potassium chloride Ca^{2+} influx ratio (red). Time course of dopaminergic neurons responding to application of 5mM KCL using FDSS 7000EX, n=2. Dotted line represents when cells were treated with ligand

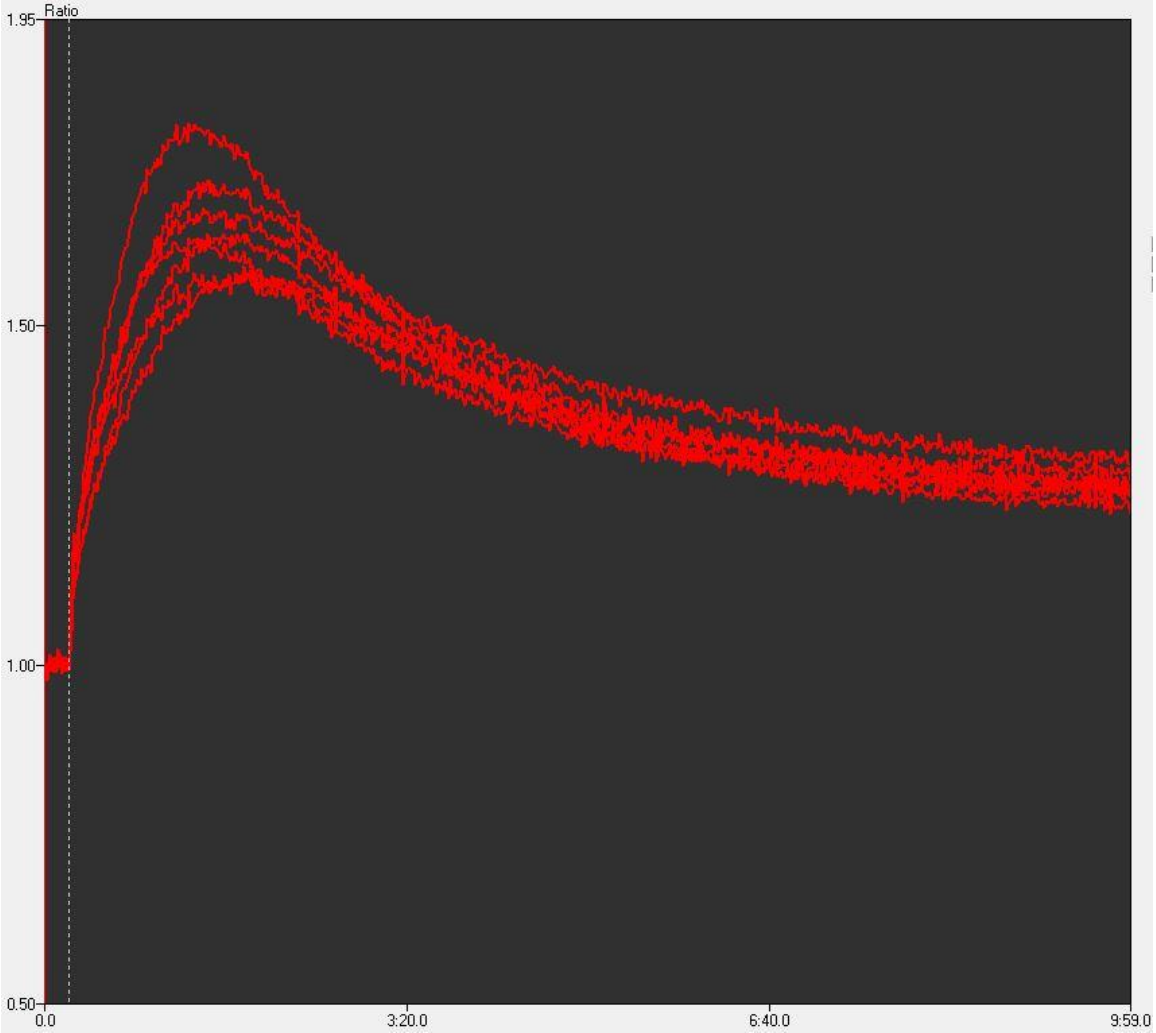

Figure 14. NMDA ligand Ca^{2+} influx

Graph representing NMDA ligand Ca^{2+} influx ratio (red). Time course of dopaminergic neurons responding to application of 250uM NMDA ligand using FDSS 7000EX. Dotted line represents when cells were treated with ligand

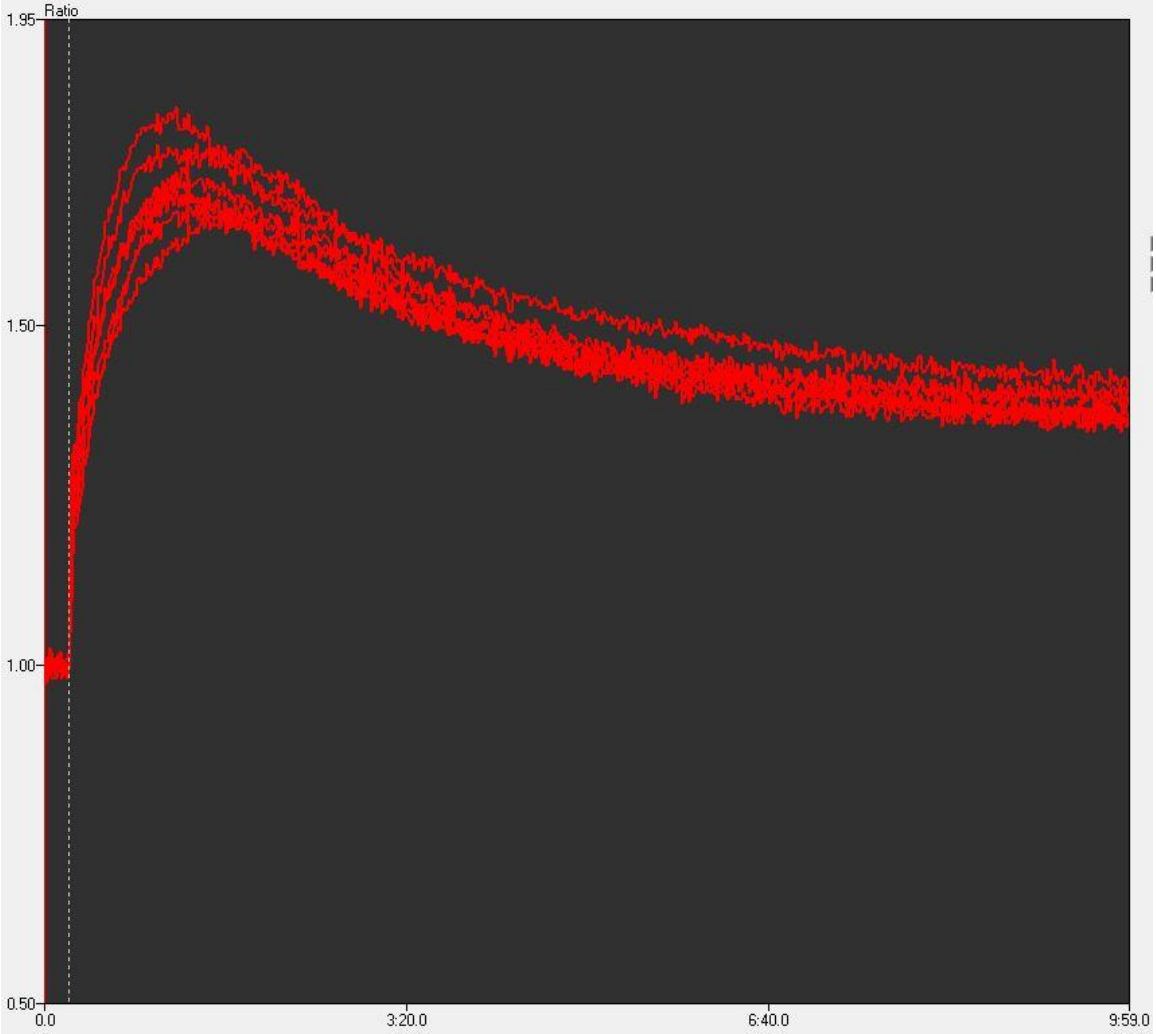

Figure 15. Ibotenic Acid Ca^{2+} influx

Graph representing Ibotenic acid Ca^{2+} influx ratio (red). Time course of dopaminergic neurons responding to application of 50uM Ibotenic acid using FDSS 7000EX. Dotted line represents when cells were treated with compound

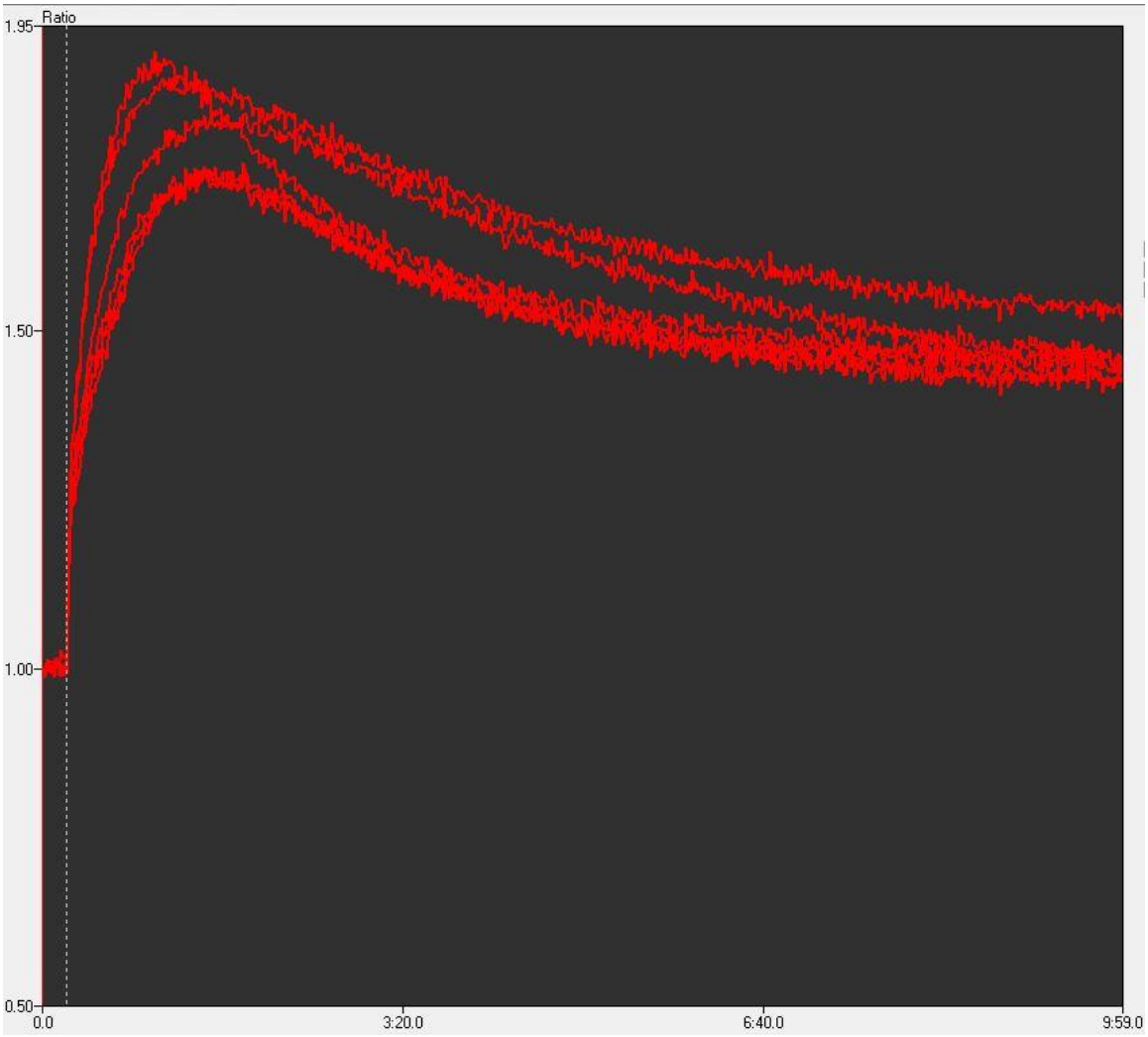

Figure 16. Kainic Acid Ca^{2+} influx

Graph representing Kainic acid Ca^{2+} influx ratio (red). Time course of dopaminergic neurons responding to application of 5mM Kainic acid using FDSS 7000EX. Dotted line represents when cells were treated with compound

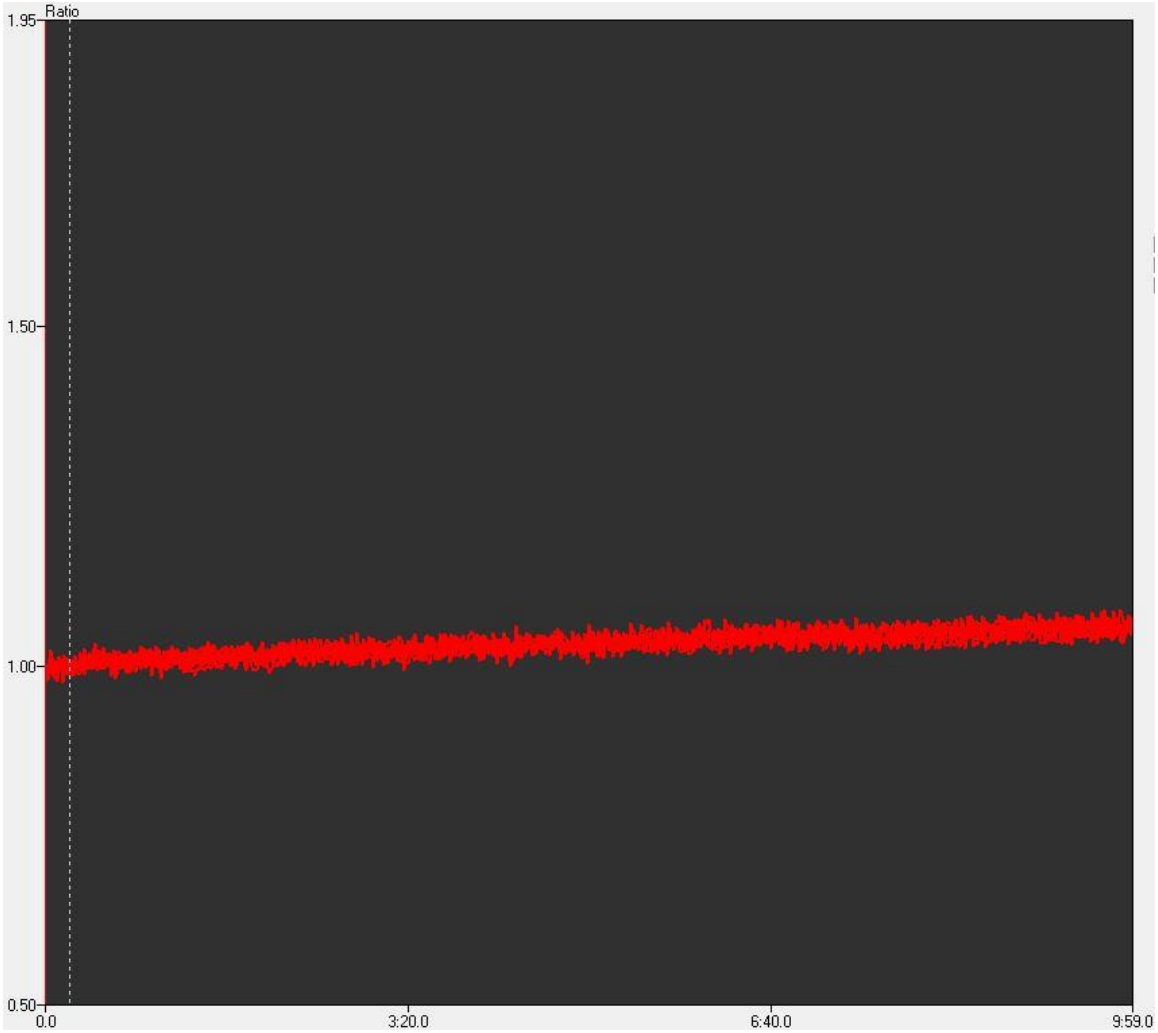

Figure 17. DMSO Ca^{2+} influx

Graph representing DMSO Ca^{2+} influx ratio (red). Time course of dopaminergic neurons responding to application of DMSO using FDSS 7000EX. Dotted line represents when cells were treated with DMSO

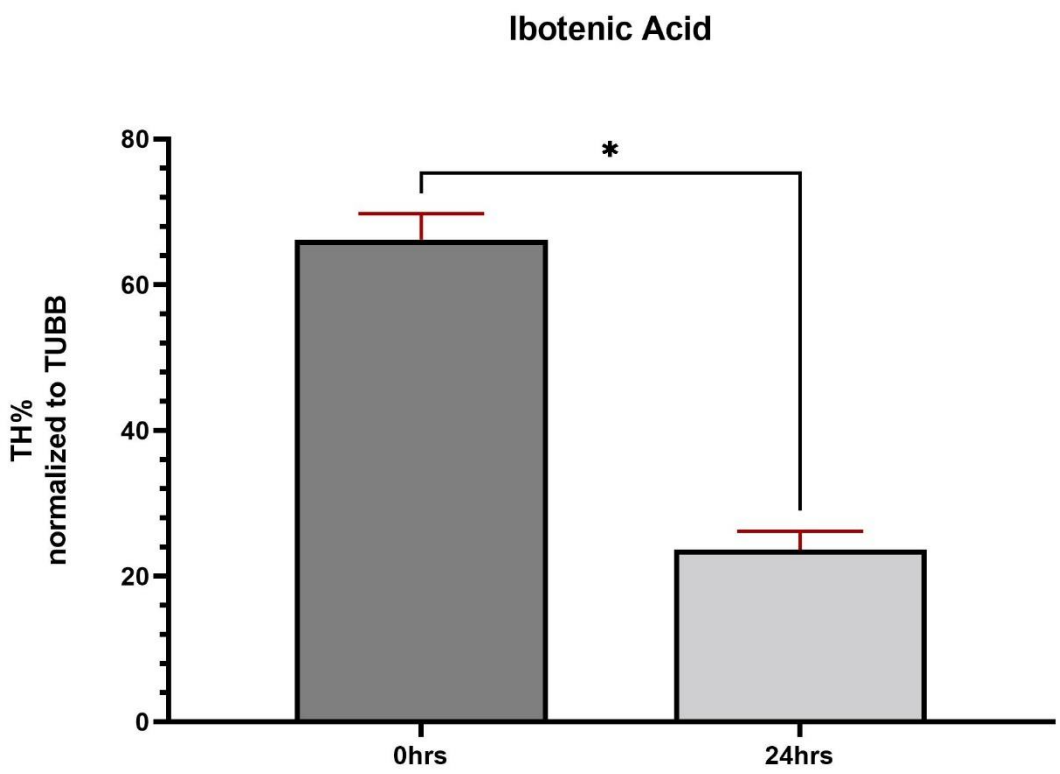

Figure 18. Ibotenic Acid excitotoxicity on TH population

*Graph representing TH levels of cells treated with glutamate agonist Ibotenic acid (50uM) for 24 hours. Cell were fix and stained with TH, normalizing to TUBB to calculate percent population of TH+ cells. The data represent the mean ± SEM. *: $p<0.05$ as assessed by one tailed Student's T test*

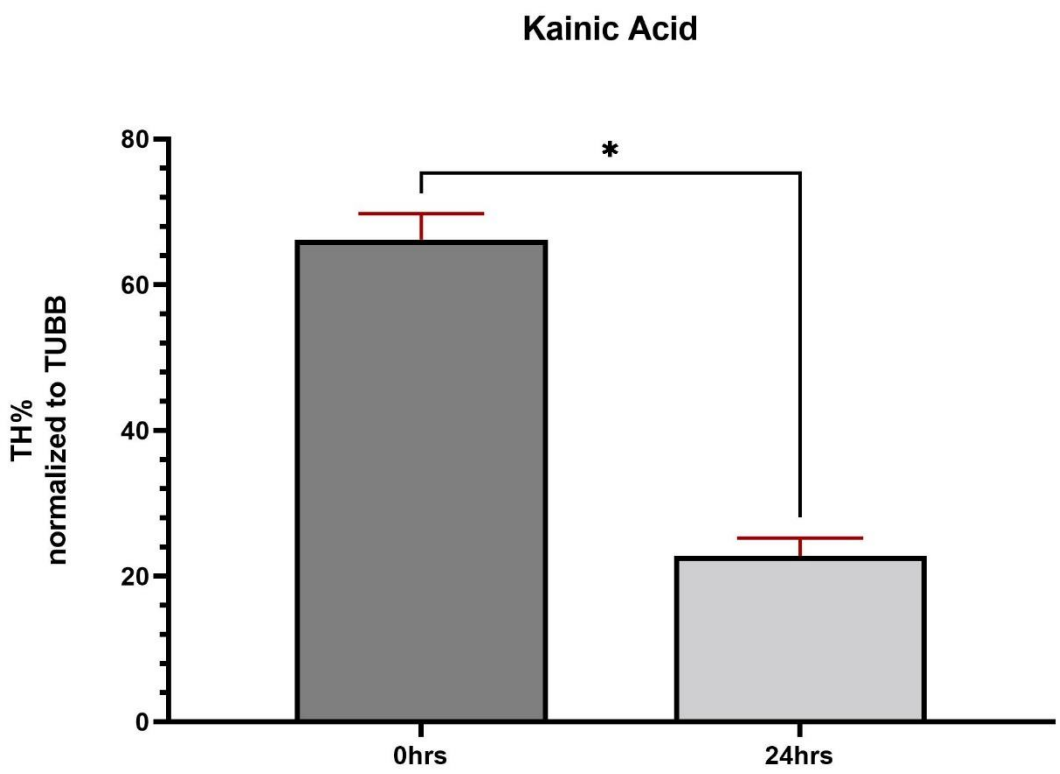

Figure 19. Kainic Acid excitotoxicity on TH population

*Graph representing TH levels of cells treated with Kainic acid (5uM) for 24 hours. Cells were fix and stained with TH, normalizing to TUBB to calculate percent population of TH+ cells. The data represent the mean ± SEM. *: $p<0.05$ as assessed by one tailed Student's T test*

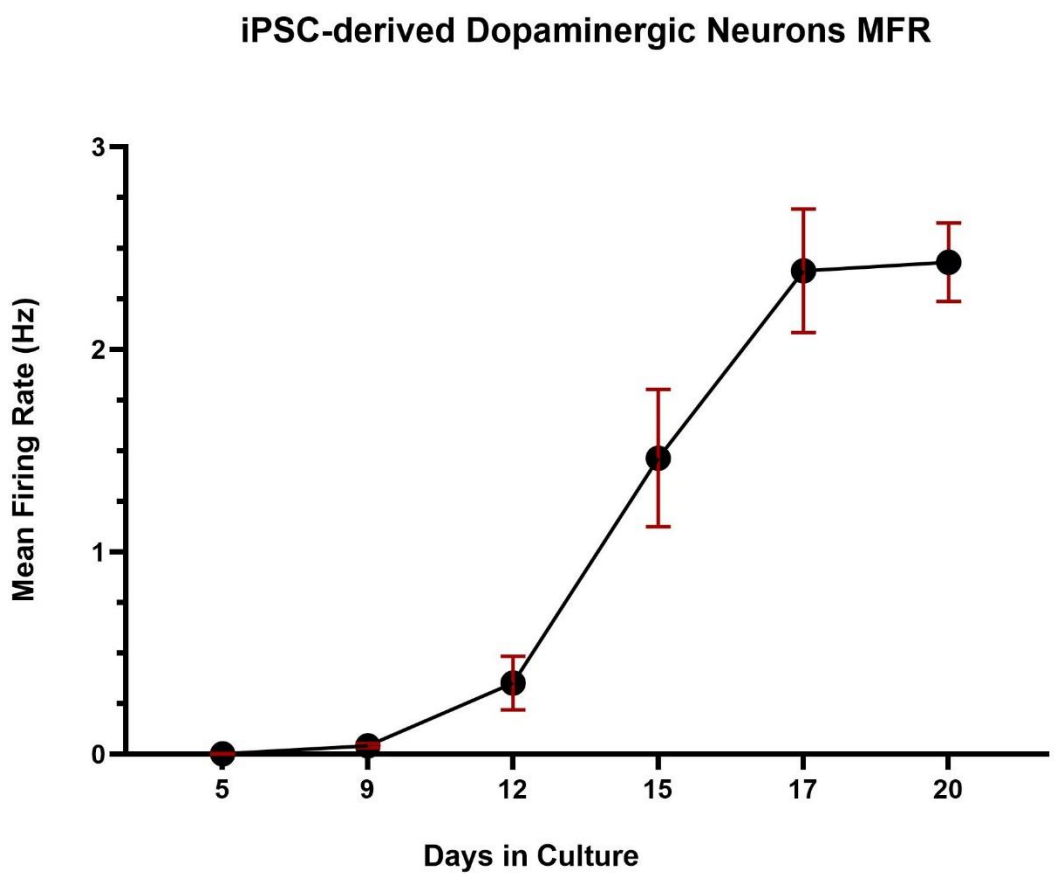

Figure 20. iPSC-derived Dopaminergic Neuron MFR

*Graph representing mean firing rate using multielectrode array assay. Cells were cultured for a period of 20 days. A 15 minutes recording was taken at day 5, 9, 12, 15, 17 and 20, n= 2. Neural Metric Tool software was used to analyze generated data. The data represent the mean ± SEM. n.s not significant, ****: p<0.0001 as assessed by One-way ANOVA*

Table 11. Ordinary one-way ANOVA multiple comparison MFR

Tukey's multiple comparisons test	Summary	Adjusted P Value
day 5 vs. day 9	ns	0.9997
day 5 vs. day 12	ns	0.1912
day 5 vs. day 15	****	<0.0001
day 5 vs. day 17	****	<0.0001
day 5 vs. day 20	****	<0.0001
day 9 vs. day 12	ns	0.2503
day 9 vs. day 15	****	<0.0001
day 9 vs. day 17	****	<0.0001
day 9 vs. day 20	****	<0.0001
day 12 vs. day 15	****	<0.0001
day 12 vs. day 17	****	<0.0001
day 12 vs. day 20	****	<0.0001
day 15 vs. day 17	****	<0.0001
day 15 vs. day 20	****	<0.0001
day 17 vs. day 20	ns	0.9996

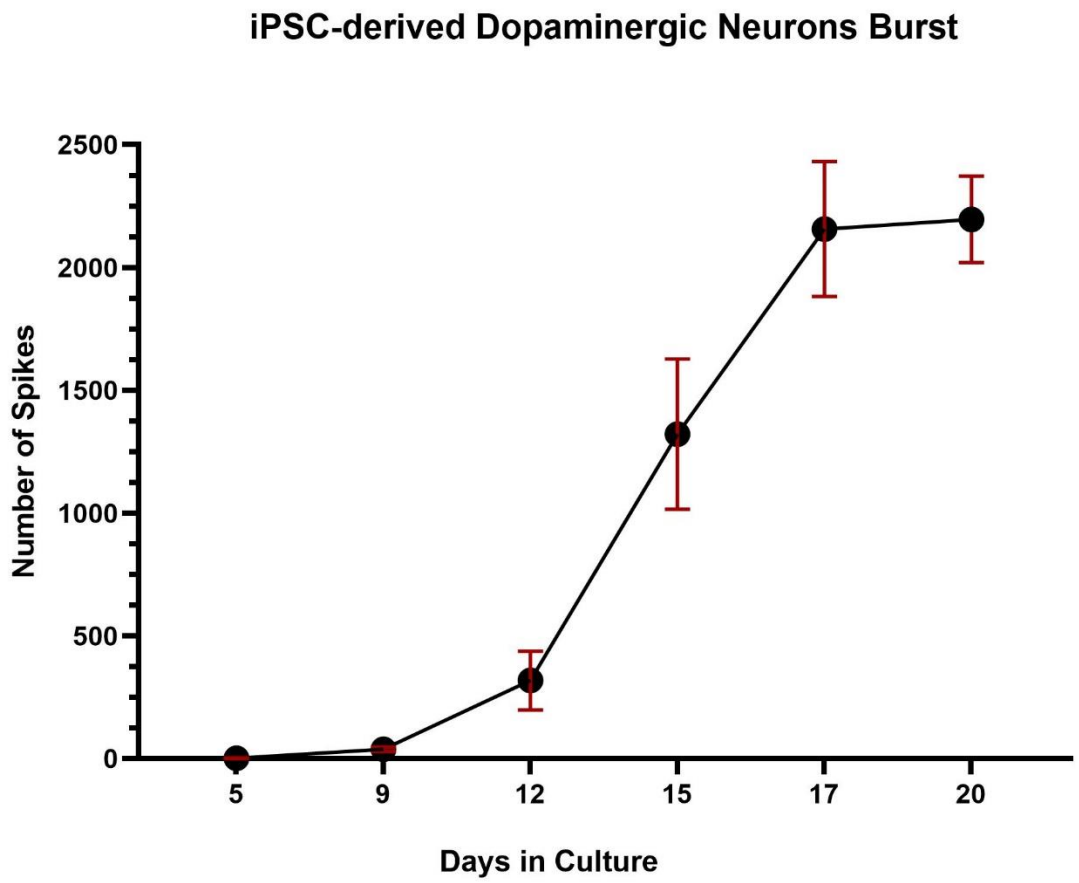

Figure 21. iPSC-derived Dopaminergic Neurons Burst

*Graph representing mean firing rate using multielectrode array assay. Cells were cultured for a period of 20 days. A 15 minutes recording was taken at day 5, 9, 12, 15, 17 and 20, n= 2. Neural Metric Tool software was used to analyze generated data. The data represent the mean ± SEM. n.s not significant, ****: p<0.0001 as assessed by One-way ANOVA*

Table 12. Ordinary one-way ANOVA multiple comparison Neuronal Burst

Tukey's multiple comparisons test	Summary	Adjusted P Value
5 vs. 9	ns	0.9997
5 vs. 12	ns	0.1899
5 vs. 15	****	<0.0001
5 vs. 17	****	<0.0001
5 vs. 20	****	<0.0001
9 vs. 12	ns	0.2486
9 vs. 15	****	<0.0001
9 vs. 17	****	<0.0001
9 vs. 20	****	<0.0001
12 vs. 15	****	<0.0001
12 vs. 17	****	<0.0001
12 vs. 20	****	<0.0001
15 vs. 17	****	<0.0001
15 vs. 20	****	<0.0001
17 vs. 20	ns	0.9995

Table 13. Phase I media components

Reagent	Stock Conc	Final Conc
Advanced DMEM/F12	1X	1X
GlutaMax	100X	1X
Pen/Strep	100X	1X
N-acetyl-cystein	0.5M	500uM
Heparin	2mg/ml	2ug/ml
N2 Supplement	100X	0.5X
SB431542	5mM	10uM
LDN193189	1mM	100nM
CHIR 99021	8mM	0.4uM
SAG	10mM	1uM
Purmorphamine	10mM	1uM

Table 14. Phase II media components

Reagent	Stock Conc	Final Conc
Advanced DMEM/F12	1X	1X
GlutaMax	100X	1X
Pen/Strep	100X	1X
N-acetyl-cystein	0.5M	500uM
Heparin	2mg/ml	2ug/ml
N2 Supplement	100X	0.5X
FGF8	100ug/mL	100ng/mL
CHIR 99021	8mM	0.6uM
SAG	10mM	1uM
Purmorphamine	10mM	1uM
Thiazovivin	10mM	1uM

Table 15. Phase III media components

Reagent	Stock Conc	Final Conc
Advanced DMEM/F12	1X	1X
GlutaMax	100X	1X
Pen/Strep	100X	1X
N-acetyl-cystein	0.5M	500uM
Heparin	2mg/ml	2ug/ml
N2 Supplement	100X	0.5X
Ascorbic Acid	200mM	200uM
FGF8	100ug/mL	100ng/mL

Table 16. Phase IV media components

Reagent	Stock Conc	Final Conc
Advanced DMEM/F12	1X	1X
GlutaMax	100X	1X
Pen/Strep	100X	1X
N-acetyl-cystein	0.5M	500uM
Heparin	2mg/ml	2ug/ml
N2 Supplement	100X	0.5X
B27 Supplement	50X	0.4X
Ascorbic Acid	200mM	200uM
Forskolin	10mM	10uM
DAPT	10mM	10uM

Table 17. Phase V media components

Reagent	Stock Conc	Final Conc
Advanced DMEM/F12	1X	1X
GlutaMax	100X	1X
Pen/Strep	100X	1X
N-acetyl-cystein	0.5M	500uM
Heparin	2mg/ml	2ug/ml
N2 Supplement	100X	0.5X
B27 Supplement	50X	1X
Ascorbic Acid	200mM	200uM
Forskolin	10mM	10uM
BDNF	100ug/ml	10ng/ml
GDNF	100ug/ml	10ng/ml

Table 18. RT-PCR Cycle Information

UNG incubation	**Polymerase Activation**	**PCR (40 cycles)**	
Hold 50ºC	Hold 95ºC	Denature 95ºC	Anneal/Extend 60ºC
2 minutes	10 minutes	15 seconds	60 seconds

References.

Arenas, Ernest. “Foxa2: the rise and fall of dopamine neurons.” *Cell stem cell* vol. 2,2 (2008): 110-2. doi:10.1016/j.stem.2008.01.012

Ball, Nicole, Teo, Wei-Peng, Chandra, Shaneel, & Chapman, James. (2019). Parkinson ’s Disease and the Environment. *Frontiers in Neurology, 10*, 218.

Bender, A., Krishnan, K. J., Morris, C. M., Taylor, G. A., Reeve, A. K., Perry, R. H., Jaros, E., Hersheson, J. S., Betts, J., Klopstock, T., Taylor, R. W., & Turnbull, D. M. (2006). High levels of mitochondrial DNA deletions in substantia nigra neurons in aging and Parkinson disease. *Nature genetics*, *38*(5), 515–517. https://doi.org/10.1038/ng1769

Behl, Tapan et al. “Cross-talks among GBA mutations, glucocerebrosidase, and α-synuclein in GBA-associated Parkinson's disease and their targeted therapeutic approaches: a comprehensive review.” *Translational neurodegeneration* vol. 10,1 4. 15 Jan. 2021, doi:10.1186/s40035-020-00226

Berardelli, A., Rothwell, J. C., Thompson, P. D., & Hallett, M. (2001). Pathophysiology of bradykinesia in Parkinson's disease. *Brain : a journal of neurology*, *124*(Pt 11), 2131–2146. https://doi.org/10.1093/brain/124.11.2131

Bonci, A, and R C Malenka. “Properties and plasticity of excitatory synapses on dopaminergic and GABAergic cells in the ventral tegmental area.” *The Journal of neuroscience : the official journal of the Society for Neuroscience* vol. 19,10 (1999): 3723-30. doi:10.1523/JNEUROSCI.19-10-03723.1999

Burré, J., Vivona, S., Diao, J., Sharma, M., Brunger, A. T., & Südhof, T. C. (2013). Properties of native brain α-synuclein. *Nature*, *498*(7453), E4–E7. https://doi.org/10.1038/nature12125

D. G. Standaert, M. H. Saint-Hilaire, C. A. Thomas (2017). Parkinson’s Disease Handbook. American Parkinson Disease Association, New York, USA

Doucet-Beaupré, Hélène et al. “Lmx1a and Lmx1b regulate mitochondrial functions and survival of adult midbrain dopaminergic neurons.” *Proceedings of the National Academy of Sciences of the United States of America* vol. 113,30 (2016): E4387-96. doi:10.1073/pnas.1520387113

Ebert, A. D., Liang, P., & Wu, J. C. (2012). Induced pluripotent stem cells as a disease modeling and drug screening platform. *Journal of cardiovascular pharmacology*, *60*(4), 408–416. https://doi.org/10.1097/FJC.0b013e318247f642

Faial, Tiago et al. “Brachyury and SMAD signalling collaboratively orchestrate distinct mesoderm and endoderm gene regulatory networks in differentiating human embryonic stem cells.” *Development (Cambridge, England)* vol. 142,12 (2015): 2121-35. doi:10.1242/dev.117838

Foster, Jane A et al. “Kainic acid lesion-induced nigral neuronal death.” *Journal of chemical neuroanatomy* vol. 26,1 (2003): 65-73. doi:10.1016/s0891-0618(03)00040-1

Gleichmann, Marc, and Mark P Mattson. “Neuronal calcium homeostasis and dysregulation.” *Antioxidants & redox signaling* vol. 14,7 (2011): 1261-73. doi:10.1089/ars.2010.3386

Hammond, C., Bergman, H., & Brown, P. (2007). Pathological synchronization in Parkinson's disease: networks, models and treatments. *Trends in neurosciences*, *30*(7), 357–364. https://doi.org/10.1016/j.tins.2007.05.004

Hynes, M et al. “Induction of midbrain dopaminergic neurons by Sonic hedgehog.” *Neuron* vol. 15,1 (1995): 35-44. doi:10.1016/0896-6273(95)90062-4

Kaur, G., & Dufour, J. M. (2012). Cell lines: Valuable tools or useless artifacts. *Spermatogenesis*, *2*(1), 1–5. https://doi.org/10.4161/spmg.19885

Le, W D, and J Jankovic. “Are dopamine receptor agonists neuroprotective in Parkinson's disease?.” *Drugs & aging* vol. 18,6 (2001): 389-96. doi:10.2165/00002512-200118060-00001

Liu, A, and A L Joyner. “EN and GBX2 play essential roles downstream of FGF8 in patterning the mouse mid/hindbrain region.” *Development (Cambridge, England)* vol. 128,2 (2001): 181-91. doi:10.1242/dev.128.2.181

Maqsood, M. I., Matin, M. M., Bahrami, A. R., & Ghasroldasht, M. M. (2013). Immortality of cell lines: challenges and advantages of establishment. *Cell biology international*, *37*(10), 1038–1045. https://doi.org/10.1002/cbin.10137

Mahul-Mellier, A. L., Burtscher, J., Maharjan, N., Weerens, L., Croisier, M., Kuttler, F., Leleu, M., Knott, G. W., & Lashuel, H. A. (2020). The process of Lewy body formation, rather than simply α-synuclein fibrillization, is one of the major drivers of neurodegeneration. *Proceedings of the National Academy of Sciences of the United States of America*, *117*(9), 4971–4982. https://doi.org/10.1073/pnas.1913904117

Michelini, E., Cevenini, L., Mezzanotte, L., Coppa, A., & Roda, A. (2010). Cell-based assays: fuelling drug discovery. *Analytical and bioanalytical chemistry*, *398*(1), 227–238. https://doi.org/10.1007/s00216-010-3933-z

Navarro-Romero, A., Montpeyó, M., & Martinez-Vicente, M. (2020). The Emerging Role of the Lysosome in Parkinson's Disease. *Cells*, *9*(11), 2399. https://doi.org/10.3390/cells9112399

Narendra, D., Tanaka, A., Suen, D. F., & Youle, R. J. (2009). Parkin-induced mitophagy in the pathogenesis of Parkinson disease. *Autophagy*, *5*(5), 706–708. https://doi.org/10.4161/auto.5.5.8505

Outeiro, T. F., Putcha, P., Tetzlaff, J. E., Spoelgen, R., Koker, M., Carvalho, F., Hyman, B. T., & McLean, P. J. (2008). Formation of toxic oligomeric alpha-synuclein species in living cells. *PloS one*, *3*(4), e1867. https://doi.org/10.1371/journal.pone.0001867

Park, Jin-Sung et al. "Mitochondrial Dysfunction in Parkinson's Disease: New Mechanistic Insights and Therapeutic Perspectives." *Current neurology and neuroscience reports* vol. 18,5 21. 3 Apr. 2018, doi:10.1007/s11910-018-0829-3

Pasinetti, G M et al. "Disappearance of GAD-mRNA and tyrosine hydroxylase in substantia nigra following striatal ibotenic acid lesions: evidence for transneuronal regression." *Experimental neurology* vol. 112,2 (1991): 131-9. doi:10.1016/0014-4886(91)90063-i

Ramirez, A., Heimbach, A., Gründemann, J., Stiller, B., Hampshire, D., Cid, L. P., Goebel, I., Mubaidin, A. F., Wriekat, A. L., Roeper, J., Al-Din, A., Hillmer, A. M., Karsak, M., Liss, B., Woods, C. G., Behrens, M. I., & Kubisch, C. (2006). Hereditary parkinsonism with dementia is caused by mutations in ATP13A2, encoding a lysosomal type 5 P-type ATPase. *Nature genetics*, *38*(10), 1184–1191. https://doi.org/10.1038/ng1884

Rienecker, Kira D A et al. "Merits and Limitations of Studying Neuronal Depolarization-Dependent Processes Using Elevated External Potassium." *ASN neuro* vol. 12 (2020): 1759091420974807. doi:10.1177/1759091420974807

Rodríguez-Traver, Eva et al. "Role of Nurr1 in the Generation and Differentiation of Dopaminergic Neurons from Stem Cells." *Neurotoxicity research* vol. 30,1 (2016): 14-31. doi:10.1007/s12640-015-9586-0

Ryan, B. J., Hoek, S., Fon, E. A., & Wade-Martins, R. (2015). Mitochondrial dysfunction and mitophagy in Parkinson's: from familial to sporadic disease. *Trends in biochemical sciences*, *40*(4), 200–210. https://doi.org/10.1016/j.tibs.2015.02.003

Scott, I C et al. "The HAND1 basic helix-loop-helix transcription factor regulates trophoblast differentiation via multiple mechanisms." *Molecular and cellular biology* vol. 20,2 (2000): 530-41. doi:10.1128/MCB.20.2.530-541.2000

Séguin, Cheryle A et al. "Establishment of endoderm progenitors by SOX transcription factor expression in human embryonic stem cells." *Cell stem cell* vol. 3,2 (2008): 182-95. doi:10.1016/j.stem.2008.06.018

Thanawala, Monica S, and Wade G Regehr. “Presynaptic calcium influx controls neurotransmitter release in part by regulating the effective size of the readily releasable pool.” *The Journal of neuroscience : the official journal of the Society for Neuroscience* vol. 33,11 (2013): 4625-33. doi:10.1523/JNEUROSCI.4031-12.2013

Waszczak, B L et al. “Effects of muscimol and picrotoxin on single unit activity of substantia nigra neurons.” *Brain research* vol. 188,1 (1980): 185-97. doi:10.1016/0006-8993(80)90567-3

Ye, W et al. “FGF and Shh signals control dopaminergic and serotonergic cell fate in the anterior neural plate.” *Cell* vol. 93,5 (1998): 755-66. doi:10.1016/s0092-8674(00)81437-3

Yin, Henry H, and Barbara J Knowlton. “The role of the basal ganglia in habit formation.” *Nature reviews. Neuroscience* vol. 7,6 (2006): 464-76. doi:10.1038/nrn1919